Published in final edited form as:
Nat Cell Biol. 2022 October ; 24(10): 1461–1474. doi:10.1038/s41556-022-00991-z.

An intercellular transfer of telomeres rescues T cells from senescence and promotes long-term immunological memory

Alessio Lanna[1,2,*], **Bruno Vaz**[#1], **Clara D'Ambra**[#1], **Salvatore Valvo**[#3], **Claudia Vuotto**[#4], **Valerio Chiurchiù**[5,6], **Oliver Devine**[7], **Massimo Sanchez**[8], **Giovanna Borsellino**[9], **Arne N. Akbar**[2,7], **Marco De Bardi**[9], **Derek W. Gilroy**[2], **Michael L. Dustin**[3], **Brendan Blumer**[10], **Michael Karin**[11]

[1]Sentcell U.K. Laboratories, IRCCS Fondazione Santa Lucia, Rome. ITALY

[2]Department of Experimental and Translational Medicine, Division of Medicine, University College London, London, London, UK

[3]Kennedy Institute of Rheumatology, Nuffield Department of Orthopaedics, Rheumatology and Musculoskeletal Sciences, University of Oxford, Oxford. United Kingdom

[4]Experimental Neuroscience, IRCCS Fondazione Santa Lucia, Rome. ITALY

[5]Institute of Translational Pharmacology, National Research Council, Rome. Italy

[6]Laboratory of resolution of NeuroInflammation, IRCCS Santa Lucia Foundation, Rome, Italy

[7]Division of Infection and Immunity, University College London, London, UK

[8]ISS, Core facilities, Rome. Italy

[9]NeuroImmunology Unit, IRCCS Fondazione Santa Lucia, Rome. ITALY

[10]Block.one, Hong Kong

[11]Laboratory of Gene Regulation and Signal Transduction, University California San Diego. USA

[#] These authors contributed equally to this work.

Abstract

[*]Correspondence should be addressed to Alessio Lanna (A.L.) alessio.lanna@sentcell.life.

Disclosure
A.L. is the Founder of SenTcell and ElecTra Life Sciences ltd. The remaining authors declare no present competing interests.

Author contribution.
A.L. conceived of, performed, and directed the study, analysed and interpreted the data, provided funding and laboratory infrastructures, formed collaborations, and wrote the paper; B.V., C.D. and C.V. designed and performed experiments and analysed individual data sets; S.V. performed lipid bilayer experiments; V.C. performed immune-phenotyping, cell-death (human) and donor cell (mouse) analysis and provided key samples; O.D. performed initial FISH and collected lymph-nodes; M.S. performed fluorescence activated vesicle sorting; M. D. B. performed APC subset isolation; A.N.A. provided initial infrastructures; G.B. performed APC subset reanalysis of telomere transfer under the guidance of A.L.; D.W.G. performed *in vivo* manipulations; M.L.D. provided lipid bilayer infrastructure, conceptual framework for synaptic vesicles, feedback and advice; B.B: inspired decentralized immunity concept and supported A.L.; and M.K. inspired A.L., provided feedback, advice, and supported experimental revisions of the final version of the manuscript, which was read, commented and approved by all authors. B.V., C.D., C.V., and S.V. contributed equally to this work.

Europe PMC Funders Author Manuscripts

The common view is that T-lymphocytes activate telomerase to delay senescence. Here we show that some T cells (primarily naïve and central memory cells) elongated telomeres by acquiring telomere vesicles from antigen-presenting cells (APCs) independently of telomerase action. Upon contact with these T cells, APCs degraded shelterin to donate telomeres, which were cleaved by the telomere trimming factor TZAP, and then transferred in extracellular vesicles at the immunological synapse. Telomere vesicles retained the Rad51 recombination factor that enabled telomere fusion with T cell chromosome ends lengthening them by an average of ~3000 base pairs. Thus, there are antigen-specific populations of T cells whose ageing fate decisions are based on telomere vesicle transfer upon initial contact with APCs. These telomere-acquiring T cells are protected from senescence before clonal division begin, conferring long-lasting immune protection.

Introduction

Telomeres are TTAGGG repeats that protect chromosome ends and promote cellular lifespan[1]. In cells with short telomeres (<4kb), proliferative activity ceases, and replicative senescence occurs rather rapidly[2]. Telomere shortening is observed in age-related pathologies, providing a common mechanism linking senescence, cancer and ageing[3]. Although cells prevent telomere shortening by telomerase-dependent and independent pathways[4,5], it is unknown whether telomeres can be transferred between cells as part of a telomere maintenance program.

Immunological synapses are excellent examples of intercellular communication formed upon antigen-specific contacts between antigen-presenting cells (APCs) and lymphocytes, and initiate immune-protective reactions that culminate with the generation of long-lived memory T-lymphocytes[6] (hereafter, T cells). Synaptic stimulation leads to activation of telomerase as part of the immune reactive response of the T cell[7]; however, repeated immune-synaptic interactions lead to a progressive decline in telomerase activation of T cells[8–11], manifestation of senescence characteristic in T cells[12–14], deterioration of immunological memory, onset of infections, cancer and eventually death.

Although certain cells, including T cells, use telomerase to temper the telomere loss consequent to their massive clonal expansion[15], telomerase activation is not sufficient to protect T cells from proliferative exhaustion, resulting in senescence of the T cells[8,12,14,16]. There is, therefore, a gap in understanding how senescent T cells are formed, and what strategies T cells employ to escape senescence and maintain long-term immunological memory instead.

We found that some T cells (primarily naïve and central memory cells) elongate their telomeres by acquiring telomeres in extracellular vesicles (EVs) from APCs. The telomere acquiring T cells become stemlike and/or central long-lived memory cells while other T cells commit to senescence. This is a hitherto unknown form of intercellular communication whereby APCs control the ageing fate of T cells during initial synaptic contacts that precede their future expansion.

Results

Discovery of telomere transfer

Telomere regulation during immune-synaptic interactions has not been studied. We used telomere restriction fragment analysis (TRF) and studied conjugates of primary human $CD27^+$ $CD28^+$ $CD4^+$ $CD3^+$ T cells (non-senescent T cells, a mixed population of naïve and central memory cells that was described previously[12,14]) and autologous APCs (peripheral blood mononuclear cells (PBMCs) depleted of $CD3^+$ T cells). We noticed T cell telomere elongation by up to 3 kb and a concurrent telomere shortening in APCs after synapse formation (Fig. 1a), in the presence of an antigen pool (Epstein Barr Virus (EBV), influenza and Citomegalovirus (CMV) lysates). Similar results were also obtained when studying immunological conjugates by confocal imaging-based telomere Fluorescence in situ hybridization (FISH) (Extended Data Fig. 1a), and qPCR (Extended Data Fig. 1b). This is in line with well recognised formation of immunological synapses in the context of antigen presentation[6,17,18].

We found that T cells deficient in telomerase (TERT-KO T cells generated by CRISPR/CAS9 transfection; Extended Data Fig. 1c-d) still elongated telomeres after exposure to APCs and antigen pool (Extended Data Fig. 1e), demonstrating that telomerase is not required for the observed telomere elongation. Telomere elongation was also not result of alternative-lengthening of telomeres (ALT)[5], a DNA break-induced recombination pathway that extends telomeres independently of telomerase, because increased telomere content was detected in T cells that are yet to divide (Bromodeoxyuridine (BrdU) based DNA assays coupled to flow-FISH; Extended Data Fig. 1f). This is suggestive of telomere elongation in the absence of DNA synthesis. Treatment with DNA polymerase inhibitors (aphidicolin and thymidine) confirmed that telomeric extension occurred even when DNA synthesis in T cells is halted (Extended Data Fig. 1g). The source of telomeres for T cell telomere elongation may have therefore be provided directly by the APCs.

Using telomere FISH, we observed that APCs presented their clustered telomeres in ~70% antigen-specific conjugates with Cell Trace Violet (CTV) labelled T cells (Fig. 1b). Clusters of molecules at the synapse often precede their transfer into the adjacent cell[17,19]. To determine if APCs are telomere donor cells, we generated a system[20] where the fluorescent Cy3 telomere PNA probes were introduced using glass beads directly into live APCs. Upon treatment, APCs did not contain any residual bead after washing (Extended Data Fig. 2a-b); but presented live-labelled telomeres that colocalized with standard telomere FISH (Extended Data Fig. 2c-d) and the protection of telomeres 1 protein (POT1; Extended Data Fig. 2e-f), demonstrating live-telomere labeling. Using this system, we visualized telomere clusters exiting APC nuclei and accumulating at the synapse with T cells (Extended Data Fig. 3a). APC telomeres are poised for cross-synaptic transfer into T cells.

We used APCs with BrdU labeled DNA and found that these APCs release telomeric DNA upon antigen-specific contacts with T cells (Fig. 1c). We also excluded that isolated T cells and APCs could spontaneously release telomeres in similar experiments (Extended Data Fig. 3b). Only trace levels of other forms of DNA, such as Alu repeats, that did not increase upon antigen challenge were detected (Extended Data Fig. 3b).

To study telomere vesicle structure, we reasoned that a system that obviates the need for antigen-specific recognition via synaptic contacts would be required. We used the calcium ionophore ionomycin, which stimulates vesicle release[21], and which was previously used to mimic synaptic dependent calcium signals triggered in APCs upon contact with T Cell Receptors (TCRs) secreted by $CD4^+$ T cells during antigen-specific immune reactions[19]. We confirmed that telomeres were included in EVs even when APCs are activated by ionomycin rather than T cells (Fig. 1d).

We then used APCs with fluorescent lipids obtained with PKH67 dye and live telomere labelling, to derive cells that release fluorescent telomere vesicles in response to ionomycin activation. Eighteen hours later, the APC conditioned supernatants were subjected to fluorescence-activated vesicle sorting (FAVS)[22]. We successfully visualised telomere vesicles within ~10% of the total APC single-particle vesicle fraction (Extended Data Fig. 3c-d). qPCR confirmed that the FAVS purified telomere vesicles contained telomeric DNA (Extended Data Fig. 3e). Vesicle free telomeres were also found, but in minor amounts (~1%; Extended Data Fig. 3f). Dot blot analysis on EV preparations further showed that telomeric DNA is mainly as double-stranded DNA molecules of small vesicle size (Extended Data Fig. 3g).

Super-resolution microscopy confirmed that membrane lipids and telomeric DNA co-localized in purified telomere vesicles released by APCs (Extended Data Fig. 3h). We also detected telomeric DNA within vesicles using transmission electron microscopy (TEM) coupled to immunogold telomere labelling (Fig. 1f and Extended Data Fig. 3i). Similar observations by field emission scanning electron microscopy (FESEM; Fig. 1g).

Next, we studied if the telomere vesicles, released by APCs, localised at the telomeres of the recipient T cells after transfer. We labelled APC DNA with 5-Ethynyl-2′-deoxyuridine (EdU), and derived FAVS-purified EdU^+ telomere vesicles from ionomycin activated APCs. We then transferred the FAVS purified telomere vesicles to separate $CD27^+$ $CD28^+$ $CD4^+$ $CD3^+$ T cell cultures not in contact with APCs, and prepared metaphase spreads 48 hours later. Strikingly, using standard FISH, we discovered that ~8% of metaphase T cell chromosome ends contained EdU labelled telomeric DNA donated by APCs (Fig. 1h; Extended Data Fig. 3j). No terminal EdU could be detected in experiments without vesicles (Fig. 1h, **top right**). Similar results using fluorescently labelled telomere vesicles such that only APC, but not endogenous T cell, telomeres could be detected (Extended Data Fig. 4a). Additionally, telomere vesicles on T cell chromosomes were destroyed upon application of T7 endonuclease that cleaves sites of DNA integration[23] (Extended Data Fig. 4b), were not immobilised on the T cell plasmalemma (Extended Data Fig. 4c), and co-immunoprecipitated with POT1 in the T cells (Extended Data Fig. 4d).

Mechanism of telomere vesicle release and recombination

Next, we studied which synapse component(s) were required for telomere transfer. Previous work described that $CD4^+$ T cells secrete the antigen receptor on[19] planar bilayers upon synapse formation of T cells on these artificial surfaces. We reasoned that APCs would release their telomeres, packaged in vesicles, on the bilayers with TCRs and an antigen pool

that induces MHC recognition (**Experimental Design**, Fig. 2a), due to similarities between ionomycin and TCR mediated activation of APCs[19].

Strikingly, telomere-labelled APCs, activated on such TCR coated planar bilayers, spontaneously released telomeres (Fig. 2b-c). The released telomeres contained APC CD63, a vesicle protein (Fig. 2b). Little release of telomere vesicles on bilayers prepared without the anti-CD3 (where T cells do not release their TCRs) or using antigen-free APCs (Fig. 2c). There is an important role of antigen-specific contacts via the TCR/ Major histocompatibility complex-II (MHC-II) to trigger telomere transfer, likely promoting calcium flux in APCs, such that pre-treating APCs with a tyrosine-protein kinase (Syk) inhibitor that blocks calcium signalling[19] prior to incubation on bilayers is sufficient to blunt telomere release on the bilayer (Fig. 2c). Telomere release was also confirmed using telomere probes and PKH67 lipid dye (Fig. 2d), brightfield illumination (Fig.2e), and isotype antibodies (Fig.2f). However, transferring ionomycin induced telomere vesicles from APCs to T cells, we found that telomere extension occurred in T cells even in the presence of MHC-II blocking antibodies (Fig.2g). MHC signalling is essential to trigger telomere transfer in physiological conditions upon antigen-specific TCR recognition, but not needed for subsequent fusion with T cell telomeres after transfer.

There was no evidence of either cell death (Extended Data Fig. 5a) or blebbing (Extended Data Fig. 5b) in ionomycin activated APCs, nor need for T cells or their receptor on the bilayers for these activated cells to release telomeres. APCs also did not die upon antigen-specific contact with T cells (Extended Data Fig. 5c). An APC subset sorting strategy revealed that myeloid APCs (Dentritic cells (DCs) and monocytes) released the highest levels of telomere vesicles while B cells released a lower amount (Extended Data Fig. 5d-e). We further assessed the composition of the telomere vesicles. Immunoblotting and ELISA determined that telomere vesicles contained vesicle and histocompatibility antigen proteins and Telomeric-zinc-finger associated protein (TZAP)[24] (Fig.3a-b), a telomere-binding protein that limits terminal ends of the chromosomes. Ionomycin-induced calcium activation increased both TZAP expression and telomere-trimming activity of TZAP immunoprecipitated from APCs assessed by TRF (Fig.3c, d), suggesting that calcium signaling stimulates TZAP activity required to generate telomeric material for subsequent vesicle transfer. In fact, TZAP-deficient APCs (Fig.3e), release little amounts of telomere vesicles upon ionomycin activation (Fig.3f-g). TZAP was also the molecule transferred at the synapse between T cells and TZAP-overexpressing APCs (Fig.3h). TZAP is involved in telomere trimming for encapsulation of telomeres into vesicles and subsequent donation to T cells.

TZAP is known to bind to telomeres that are deprotected of shelterin proteins[24], a telomere-binding complex that protects telomeres from the DNA damage response, ensuring telomere stability. We found that APCs, ionomycin activated or in synapse with T cells, down-regulated expression of both telomere-binding and shelterin-assembling factors, POT1 and (Telomeric repeat binding factor 2) TRF2[25,26], that was evident by confocal imaging of ionomycin activated APCs (Fig. 4a) and immune conjugates (Fig. 4b) and immunoblotting of isolated APCs upon ionomycin activation (Fig. 4c). By contrast, shelterin down-regulation was prevented in APCs treated with proteasome inhibitor MG-132- prior to

synapse with T cells (Fig. 4b), suggesting that APC shelterin undergoes calcium-dependent proteasomal degradation upon antigen-specific contacts with T cells[27]. Therefore, both ionomycin activation and synapse formation events result in similar degradation of shelterin proteins that precedes telomere transfer.

Surprisingly, confocal imaging revealed that telomere-shelterin co-localization was not absolute in APCs (Fig. 4a). Although the reason for absence of shelterin on some APC telomeres is not clear, it is possible that some APC telomeres may be naturally devoid of shelterin due to prior episodes of telomere transfer *in vivo* and/or baseline activation by the culture conditions *per se*. We therefore tested if shelterin may had been lost to induce telomere vesicle release from APCs. Immunofluorescence analysis of shelterin proteins revealed that telomere vesicles did not contain TRF2 or POT1 (Fig. 4d). Enforcing shelterin levels in APCs by POT1/TRF2 co-transduction (Extended Data Fig. 6a), suppressed release of telomere vesicles from APCs stimulated by ionomycin (Fig. 4e). Conversely, global demolition of shelterin (Extended Data Fig. 6b) was sufficient to induce spontaneous telomere vesicle release even from resting APCs (Fig. 4f). The effects of shelterin modulation on APC vesicle release were confirmed and quantified by FAVS (Fig. 4g-h). Shelterin proteins prevent telomere transfer, and once these proteins are degraded, TZAP can lead to telomere excision and release in EVs.

Immunofluorescence revealed that telomere vesicles retained Rad51, the homologous recombination factor involved in telomere elongation[28] (Fig. 5a). Immunoblot analysis on the vesicle preparations further confirmed presence of other DNA damage factors in ultracentrifuged supernatants where the Rad51+ telomere vesicles are found (Fig. 5b).

We reasoned that Rad51 may be required for telomere recombination upon vesicle transfer. We silenced Rad51 in APCs (Fig.5c) and found that telomere vesicles depleted of Rad51 retained vesicle count (Fig. 5d), size (Fig. 5e) and key telomere vesicle molecules (Fig. 5f). However, the Rad51-depleted vesicles had reduced presence of repair factor BRCA2 (Fig. 5f) and single strand telomere DNAs (Fig. 5g), suggesting impaired recombinogenic potential. To test if telomere vesicles depleted of Rad51 were defective at recruitment at T cell telomeres, we live-labelled Rad51-deficient APCs with Cy3 fluorescent TelC telomere probes, derived fluorescent APC telomeres (labelled in red) by ionomycin activation, then transferred the APC supernatants containing the fluorescent telomere vesicles into separate T cell telomere nuclei, labelled in green. Twenty-four hours later, we found that telomere vesicles depleted of Rad51 had impaired co-localisation with T cell telomeres, in notable contrast with telomere vesicles that possess Rad51 (siCtrl *vs* siRad51; Fig. 5h). Furthermore, upon transfer, these Rad51 deficient vesicles generated T cell chromosome ends that were ~1.2kb shorter compared to those fusing with vesicles that possess Rad51 (Fig. 5i). This was not due to a defect in telomere vesicle release by RAD51-deficient APCs (Fig. 5d), neither due to a difference in absolute telomere length between Rad51-deficient and control telomere vesicles as shown by TRF performed directly on the vesicles (Fig. 5j). We also found evidence of disrupted T cell telomere elongation upon transfer of Rad51-deficient telomeres vesicles compared to control telomere vesicles that possess Rad51 by qPCR (Fig. 5k). Telomere vesicle transfer extends individual T cell chromosome ends, and Rad51 in the vesicles is required for the telomere extension reaction.

Europe PMC Funders Author Manuscripts

Generation of long-lasting immunity by telomere transfer

A significant limit of *in vitro* T cell expansion protocols is accelerated senescence of the T cells observed in immunological cultures [8,13,14,29,30]. Nonsenescent T cells activated in the presence of control telomere vesicles expanded ~3 fold more, over 30-40 days, compared to cells left without any vesicles or stimulated with telomere depleted vesicles or even telomere vesicles depleted of Rad51 (Fig. 6a). In similar experiments with a single activation of T cells, vesicle free telomeres were ineffective (Extended Data Fig.7a). In these experiments, similar expansion was obtained using heterologous human vesicles and even mouse vesicles. Telomere vesicles were also superior in supporting the proliferative expansion of T cells in culture than telomerase over-activation by CRISPR/Cas9 activation (Extended Data Fig.7b-c). Telomere vesicles also supported the proliferation of TERT-KO T cells in similar experiments (Extended Data Fig.7d). We also assessed nonsenescent T cells that received TZAP-deficient telomere vesicles and found they proliferated poorly compared to T cells containing telomere vesicles derived from control (TZAP-expressing) APCs (Extended Data Fig. 7e), consistent with TZAP-deficient APCs releasing a lower vesicle amount rather than a functional defect *per se*. A transfer of vesicles over-expressing TZAP containing $TZAP^+$ vesicles produced the opposite effect (Extended Data Fig. 7f).

We next measured ultra-short telomeres and found that telomere vesicle transfer, but not telomerase over-expression, nearly eliminated the burden of ultra-short telomeres in non-senescent T cells (Extended Data Fig. 7g). Therefore, even T cells that are yet to be senescent contain some ultra-short telomeres, and these cells may be fated to senescence in the future if they do not receive adequate support from telomere vesicle transfer when an antigen-specific immunological synapse event occurs.

We therefore tested if telomere vesicle transfer would protect T cells from replicative senescence. Markers of cellular senescence (beta-gal and sestrin) were abrogated in T cells grown with telomere vesicles compared to those T cells cultured with telomere-depleted vesicles or telomere vesicles depleted of Rad51, or left without any vesicles after a ten-day culture (Fig. 6b and Extended Data Fig. 8a,b). Phenotypic modulation in primary human $CD4^+$ T cells was by both human and mouse vesicles, suggestive of evolutionary-conserved immune-rejuvenation (Extended Data Fig. 8c,d).

Strikingly, in fact, conversion of naïve $CD45RA^+$ $CD28^+$ $CD4^+$ T cells to $CD28^-$ $CD4^+$ T cells, a highly differentiated end-stage population of cells that possess many senescent features in humans[8,13,29–33], was also strongly reduced by telomere vesicles (Fig. 6c). Prevention of senescence led to enhanced generation of $CD28^+$ $CD62L^+$ $CD45RA^+$ $CD95^+$ stem-like memory T cells[34] from highly purified naïve-T cell populations exposed to telomere vesicles during a 15-day culture (Fig. 6d, left. **middle and right panel**). The proportion of $CD28^+$ $CD45RA^-$ central memory cells upon transfer of telomere vesicles was also increased (Fig. 6d, **left panel**).

Naive and central memory cells were the major telomere acquiring T cells from APCs upon antigen pool stimulation (Extended Data Fig. 9). By contrast, effector $CD28^-$ T cells, especially $CD28^-$ $CDRA^-$ effector memory cells, and to a lesser extent $CD28^-$ $CDRA^+$ terminally differentiated effector memory cells T cells (EMRA; with relatively higher

telomere length than EM), which both contain a substantial proportion of end-stage poorly proliferative senescent T cells, exhibited reduced telomere acquiring capacity. Therefore, only some populations of T cells are able to acquire telomeres from APCs to escape senescence.

We next studied telomere transfer *in vivo*, using an OT-II Ovalbumin (OVA)-antigen specific system. We injected OVA-loaded APCs in the footpad of recipient animals, with intravenous injection of CTV labelled OT-II T cells 18 hours later, and collected sub-popliteal lymph nodes after additional 18 hours (Fig. 6e). We found that ~50% OT-II T cells had acquired telomeres from OVA-pulsed APCs with minimal, if any, telomere transfer in the absence of OVA (Fig. 6f). We also confirmed that APC telomeres resided in T cell nuclei upon telomere transfer *in vivo* (Fig. 6g). Similar observations by *in vivo* APC DNA labelling with Edu through a drinking water protocol, followed by synapse formation between Edu-labelled APCs and EdU-free (congenic) OT-II in the presence of OVA (Extended Data Fig.10a).

Next, we assessed the effect of telomere transfer *in vivo* using a CD45.1/2 T cell tracking system. We derived CD45.2 OT-II $CD4^+$ T cells that had acquired telomeres upon synapse with OVA-pulsed TelC-labelled APCs (Extended Data Fig.10b) and injected them into CD45.1 recipients, followed by recipient vaccination 18 hours later. As a control, we injected identical amounts of CD45.2 OT-II $CD4^+$ T cells that did not acquire telomeres in the same synaptic process and performed identical recipient vaccination. Five days post-vaccination with OVA, T cells with APC telomeres expanded significantly more than those that did not acquire telomeres (Fig. 6h), showing that telomere transfer supports antigen-specific proliferative expansion of T cells.

In parallel longevity experiments, we performed a second OVA vaccination 40 days after transfer. Fifty days after the second vaccination, we observed these T cells with APC telomeres in increased proportions than those injected without APC telomeres in both spleens and lymph nodes (Fig. 6i). Similar to naive human T cells with APC telomeres, these mouse T cells also had elevated expression of CD95, even in the naïve T cell compartment ($CD62L^+$ $CD44^-$), resulting in an increased stem-like T cell memory switch (Fig. 6j, **bottom**). Central memory cells were also increased (Fig. 6j, **top**). By contrast, mouse T cells without APC telomeres had reduced CD95 and CD62L expression but expressed increased CD44 levels, suggesting generation of $CD44^{high}$ senescent mouse T cells[35,36] or their progenitors *in vivo* (Extended Data Fig.10c-d). No enrichment of T cells with APC telomeres could be observed in the blood of vaccinated mice (Extended Data Fig.10e-f). T cells with APC telomeres may migrate rapidly to long-term reservoirs, to maintain long-term immunological memory

We next tested the role of vesicle Rad51 *in vivo*, providing resting CD45.2 OTII $CD4^+$ T cells with purified telomere vesicles that possess, or not, Rad51 prior to injection in CD45.1 recipients and vaccination with OVA (Fig. 7a). After two rounds of vaccination, we observed similar enhanced long-term T cell presence (70 days) in these adoptive transfer experiments with ionomycin based telomere vesicle extraction rather than cross-synaptic transfer of telomeres (Fig. 7b-c). However, these effects were not observed if the transferred CD45.2 T cells were supplemented with telomere vesicles depleted of Rad51 (Fig. 7b-c).

Phenotype modulation also required Rad51 in the vesicles (Fig. 7d). Rad51 present in the telomere vesicles is required for T cell longevity effects in both human and mouse systems.

Finally, we tested the role of telomere vesicles in immune defense using a previously published FLUAD influenza vaccination protocol of mice[12]. Five days post vaccination, FLUAD-primed T cells were treated with APC telomere vesicles, or telomere depleted vesicles then intravenously injected into naïve congenic recipients that were not immunized with FLUAD vaccines. Recipient mice were then infected with H1N1 influenza viruses either 18 hours after injection, or 15 days later, to assess the long-term immune protection characteristic of memory phase that is important to prevent later infections (Fig. 8a). While control mice that received unvaccinated T cells died rapidly upon infection, short-term immune protection was similar between mice receiving either T cells with telomere vesicles or telomere depleted vesicles (Fig. 8b). However, only animals that received primed T cells with telomere vesicles survived delayed infection after 15 days of injection (Fig. 8c). Telomere vesicle transfer can be used to reinforce long-term immunological memory at the point of immunisation.

Discussion

How senescent T cells are formed remain poorly understood. We propose a model whereby telomere transfer from APCs protects the recipient T cells from replicative senescence. The recipient is preferably a naive or central memory T cell. When recipient T cells acquire telomeres from APCs during antigen presentation, they shift towards a stem-like/central long-lived memory state. Failure to acquire telomeres skews them towards senescence instead.

Although our model describes that the ageing fate of some T cells is determined well-before cell division begin, additional pathways to memory T cell generation exist. For instance, memory T cells may form linearly upon contraction of an immediate effector response and metabolic switch from glycolysis towards oxidative phosphorylation[37]; alternatively, the memory cell may arise directly from the naïve one bypassing an effector state through a process of asymmetric division[38]. It is also possible that discrete populations of T cells with stem-like properties originate all forms of memory cells[39].

It is not clear how T cells with APC telomeres will divide upon telomere transfer, however, these T cells may subsequently divide and differentiate both linearly[40] and/or asymmetrically[41] after antigen stimulation, if telomere transfer occurs. It is possible that antigen strength may affect the amount of telomere transfer and subsequent division of T cells. However, even in situations where antigen specificity was identical, a large proportion of T cells still failed to acquire telomeres from APCs, shifting towards a short-lived effector state; some of these cells may serve as senescent progenitors. Therefore, additional mechanisms controlling telomere transfer during antigen presentation beyond TCR specificity would have to exist.

It is believed that T cells become senescent after repeated episodes of antigen-stimulation[15], when highly-differentiated effectors fail to further activate the telomerase, and proliferative

Europe PMC Funders Author Manuscripts

activity ceases. Such linear senescence pathway is possible, and T cells that do not receive telomeres can certainly proliferate, albeit to a lower extent than those T cells that do receive telomeres; however, our results support an alternative model for senescent T cell generation whereby only one failed round of telomere transfer during antigen stimulation destines T cells towards senescence in the future. We propose that both telomerase and the here described telomere transfer process co-operate to support T cells at two different points in the activation of the T cell. Telomere transfer occurs when T cells are still bound to APCs and form immunological synapses during an antigen-specific process, then telomerase acts after the synapse dissolves and the T cells undergo massive proliferative expansion instead. Thus, while telomerase replenishes telomere loss at all chromosomes during post-synaptic T cell divisions (~100-200 bp), telomere transfer augments certain, likely ultra-short, telomeres by ~3,000 before cell division begin.

In conclusion, our data describe fundamental ageing fate decisions of T cells being made immediately, during initial synaptic contacts with APCs, pending telomere transfer. It was suggested previously that as yet undefined signals must be responsible for terminal differentiation and senescence of T cells[42]. We now propose telomere transfer to be that signal. This is different from senescent T cells being thought to accumulate during chronic viral infections, natural ageing, and cancer[11,15,43] because unlike T cells with APC telomeres, these cells do not possess the ability to undergo antigen-specific expansion. Controversy is present on whether senescent T cells may be resistant[44] or prone to apoptosis[45] and what is the underlying mechanism leading to their generation. We suggest that senescent T cells, or their progenitors, may be short-lived cells that are continuously generated by episodes of activation that lack telomere transfer. An important but as yet undefined function of the immunological synapse is, therefore, immediate determination of senescence fates of T cells. This model does not exclude that memory cells may also derive from effector cells via a process of de-differentiation[46], and those de-differentiated cells also have stem-like features[46] similarly to the T cells with APC telomeres.

The intercellular telomere transfer reaction described is a different form of decentralized immunity[47] whereby APCs distribute telomeres to favour some T cells becoming long-lived memory cells, bypassing senescence. Decentralisation indicates T cells do not rely just on a single molecule, telomerase, to extend telomeres. Whether the memory T cells generated in the absence of telomere transfer have the same longevity outlook than those telomere-acquiring T cells we have studied remains to be determined.

Materials and Methods

Human and mouse studies

This research complies with all relevant ethical regulations. All human specimens were obtained with the approval of Fondazione Santa Lucia Ethical Committee or the Ethical Committee of Royal Free and University College Medical School or the University of Oxford, with voluntary informed consent in accordance with the Declaration of Helsinki. No compensation was offered to any participant. For mouse studies, we received approval from the Italian Ministry of Health or the UK Home Office to undertake work at Fondazione Santa Lucia or the University College London. Mouse husbandry was controlled by standard

circadian rhythms (12 hours of dark and 12 hours of light; fixed temperature 25°C, humidity between 40-60%). For human studies, age (20-65) and sex (male 55% and female 45%) were uniformly distributed across experiments. All antibodies used in this study are enlisted in Supplementary Table 2. Immune analyses were carried with CytExpert (V2.4) or FACSdiva software (V8.0.0.1).

Cell isolation

Primary human nonsenescent $CD3^+$ $CD4^+$ $CD27^+$ $CD28^+$ T were purified using commercially available kits from Miltenyi (CD4 T cell isolation kit 130-096-533; CD27 microbeads first (130-051-601; from peripheral blood mononuclear cells (PBMCs) previously isolated by Ficoll of healthy volunteers as described previously[1] and used throughout all human experiments. For isolation of primary mouse $CD4^+$ T cells from splenocytes, CD4 MicroBeads (L3T4; 130-117-043) were used. For APC purification (CD3-depleted PBMCs; or CD3-depleted autologous mouse splenocytes), human CD3 MicroBeads (130-050-101) and mouse CD3e Microbead kit (130-094-973) were used to deplete T cells, all from Miltenyi.

Cells Immunoblotting

Cells were lysed in 50 ml RIPA buffer (R0278; Sigma-Aldrich) supplied with 1x protease and phosphate inhibitors. The cell-lysis mix was incubated for 20 mins on ice and centrifuged for 20 min at the max speed (15,871g) at 4°C. Cell extracts were separated on polyacrylamide gel, then fast transferred to nitrocellulose membranes with Trans-Blot machine (Biorad). Membranes were washed with 0.1% Tween-TBS buffer and blocked in 5% non-fat milk for 1hr followed by incubation with the primary antibodies (1:1000, Cell signalling) overnight at 4°C, washed again, then incubated with secondary antibody (1:5000, Cell signalling 7074P2 or 12-349, Sigma-Aldrich). ECL solution (A38554 ThermoFisher) was used for developing at Chemidoc (iBright1000, Thermofisher).

Signalling studies

Telomere vesicles were stained with antibodies to Rad51 (1:100; ab63801, Abcam) and TRF2 (1:300; ab13579, Abcam) and POT1 (1:300; PA-66996, ThermoFisher). Primary human T cells were stained with antibodies to sestrin 1 (1:300; ab134091, Abcam). Shelterin expression in primary human APCs was evaluated with antibodies to TRF2 and POT1 as per telomere vesicles. APCs were also stained with TZAP (H00003104-B01P, Novusbio), Caspase 3 (9661T, Cell Signaling) and H3, (ab18521, Abcam).

Shelterin modulation

Primary human APCs were cultured with GMCSF (10ng/ml; Merck GF304) and IL-4 (50ng/ml; Miltenyi 130-093-922) for 48h, then transduced with POT1 (sc-403275-LAC) and TRF2 (sc-401289-LAC) lentiviral activation particles (both from Santa-Cruz Biotechnology) at multiplicity of infection (MOI) of 10. Control APCs were transduced with control lentiviral activation particles (sc-437282-lac, Santa Cruz Biotechnology). For IF-FISH to POT1 we used either NB500-176 (Novusbio) or PA-66996, (ThermoFisher) (both at 1;300 dilution), with similar results. Conversely, shelterin-deficient APCs were generated

by siTRF2 (sc-38505, Santa Cruz Biotechnology) plus siPOT1 (sc-44032, Santa Cruz Biotechnology) nucleofection.

Telomerase modulation by CRISPR

Primary human $CD3^+$ $CD4^+$ $CD27^+$ $CD28^+$ T cells (5 x 10^6) were transfected with 3mg of TERT KO CRISPR/Cas9 plasmid (h) (sc-400316, Santa Cruz Biotechnology) according to the manufacturer instructions. TERT-KO (GFP^+) T cells were then activated by anti-CD3 (0.5 μg/ml; OKT3 86022706 Sigma Aldrich used throughout) plus anti-CD28 (0.5 μg/mL; 37407 MAB342 R&D systems used throughout) and then purified by FACS 96h post-transfection. Control primary human $CD3^+$ $CD4^+$ $CD27^+$ $CD28^+$ T cells were transfected with 3mg of control CRISPR/Cas9 Plasmid (sc-418922, Santa Cruz Biotechnology). Knock-out efficiency was confirmed by qPCR (Hs00972656_m1; TaqMan). Transcript expression was normalized to that of the housekeeping gene *GAPDH* by the change-in-cycling-threshold method (ΔΔCt) for the calculation of values supplied by Applied Biosystems. In experiments with telomerase enhancement, 10^7 primary human $CD3^+$ $CD4^+$ $CD27^+$ $CD28^+$ T cells were transfected with 3 μg of CRISPR telomerase activation particles (sc-400316-ACT, Santa Cruz Biotechnology) and then used 96h post transfection. For immunoblots to TERT (1:1000; sc-7212, Santa Cruz Biotechnology) on purified GFP^+ primary human T cells was used as previously described[1]. Control was control CRISPR/Cas9 Plasmid as advised by the manufacturer (sc-437275, Santa Cruz Biotechnology).

Telomere Immunofluorescence *In situ* hybridization FISH (IF-FISH)

Sections were spun 5 minutes at 300g on imaging coverslips. Sections were then dried, fixed in ice-cold 3.7% formaldehyde for 15 min, washed in PBS and treated 20 min with -20°C ethanol. Blocking was performed for 1 h at room temperature in PBS-TT (8% BSA, 0.5% Tween-20 and 0.1% Triton X-100 in PBS). Primary stainings were performed overnight at 4°C with antibodies to TRF2 and POT-1 (1:300; Abcam and ThermoFisher,); CD3 (1:1000; BIO-RAD MCA463G). Secondary stainings were performed for 1 h at room temperature in the dark with biotinylated goat anti-rabbit IgG AlexaFluor 405 (1:400; A-31556, Life Technologies) and goat anti-mouse IgG1 AlexaFluor 647 (1:800; Life Technologies A-21240, Life Technologies). Cross-linking was performed 20 min in 4% paraformaldehyde. Sections were dehydrated in graded ethanol (70%; 90%; 100%), treated with DNase-free RNase (100 ng/mL; Thermofisher) for 60 min then hybridized with 40 pM PNA probe solution (Panagene, TelC Cy3, 14 1224PL-01) in hybridization buffer (1M Tris pH 7.2; magnesium chloride buffer; deionised formamide; blocking buffer, Roche; deionised water). DNA denaturation was performed 10 min at 82°C. Hybridisation was allowed 2 h at room temperature, followed by subsequent washing in 70% formamide, saline sodium citrate (SSC) buffer and PBS, respectively. DNA was stained for 5 min in PBS with 1 μg/ml of DAPI and coverslips mounted with Pro-Long Gold (Invitrogen). Imaging was performed using a Leica SPE2 confocal microscope using LAS X version 3.3.0 software (Leica Microsystems, Wetzlar, Germany) or super-resolution ZEISS LSM 800 Airyscan (Zeiss) using Zen lite software version 2.3. Sections were z-stacked and the average telomere integrated fluorescence per cell nucleus was quantified by ImageJ software (V2.1).

Antigen-specific conjugates

Human APCs were pre-pulsed for 4h at 37°C with 1:50 antigen pool (EBV, CMV, influenza lysates, Zeptometrix) or 1:50 cytomegalovirus (CMV)-lysates (Zeptometrix Corporation; for initial IF-FISH studies). Primary human APC-T cell conjugates were formed in a 3:1 ratio, spun at 300g for 5 min, then incubated at 37 °C as indicated. For time course experiments using immunological conjugates (e.g. in IF-FISH), APCs and T cells were allowed in culture for 20 min after spinning on coverslips prior to analysis. This first analysis time point was considered time 0, to account for immune synapse formation *in vitro*.

Isolation of extracellular vesicles (EVs) by ultracentrifugation

Vesicles were isolated from APC supernatants activated with ionomycin (0.5 μg/ml) or upon antigen specific contact with $CD3^+$ $CD4^+$ $CD27^+$ $CD28^+$ T cells following sequential centrifugation (300g 10 min; 2,000g 10 min; 10,000g for 30 min). Where indicated, the 10,000g centrifuged APC supernatants were further passed through 0.3 μM filters to remove vesicle clusters, and EVs pelleted at 100,000g for 90min to derive vesicle-enriched preparations.

Vesicle Immunoblotting

Pellets obtained after each sequential centrifugation step were resuspended in PBS and used for vesicle immunoblotting with the primary antibodies used in ELISA applications (see below) plus p-H2AX S139 (ab26350, Abcam) and BRCA1 (GTX70113, GeneTex). Input was 20% APC whole cell lysates. Fractionation purity was confirmed with antibodies to cytochrome C (556432, BD pharmigen). Antibodies were used at 1:1000 dilution.

Generation of APCs with fluorescent telomeres

APCs were adhered overnight on glass coverslips in complete RPMI-1640 medium (supplemented with 10% heat-inactivated FCS, 100 U/ml penicillin, 100 mg/ml streptomycin, 50 μg/ml gentamicin, and 2 mM L-glutamine). Cy-3 TelC PNA probes were dissolved 1:50 in telomere loading buffer (80 mM KCl, 10 mM K_2PO_4, 4 mM NaCl, pH 7.2) and gently introduced on adherent live-APCs by rolling pH 7.2 alkali pre-washed large (400-600mM) glass-beads (G8772, Sigma Aldrich) for 5 min as previously described[20]. Alkali bead washing was performed overnight in 1M NaOH. TelC-Cy3-probe labelled APCs were washed in PBS twice after rolling, and cultured in complete RPMI.

Fluorescence activated vesicle sorting

Fluorescent telomere vesicles (PKH67+ TTAGGG+ single particles) were depleted by MoFlo Astrios-EQ flow cytometer (Beckman Coulter) equipped with 5 lasers (355, 405, 488, 561 and 640 nm wavelengths). To reduce instrument background noise, the system is also equipped with inline sheath filter with 40 nm pore size. The applied pressure to sheath fluid was 60 psi. Routinely alignments were performed with Ultra Rainbow Fluorescent Particles 3.0 μm (URFP-30-2, Spherotech). The triggering threshold was applied to the side scatter on the 488-SSC channel and the relative applied voltage was determined by using size reference beads (1493, Apogee flow systems) to exclude vesicle aggregates >300 nm. The Instrument setup to identify microvesicles was obtained by balancing triggering

threshold and SSC voltage in order to reduce and maintain over time the background noise at 150-300 events/sec.

Fluorescence activated vesicle release analysis of primary human APC subsets

Primary human DCs ($CD3^-$ $CD56^-$ $CD19^-$ $HLADR^+$ $CD16^-$ $CD14^-$ $CD11C^{+/-}$ $CD123^{+/-}$); or B cells ($CD3^-$ $CD56^-$ $HLADR^+$ $CD19^+$) or monocytes ($CD56^-$ $CD19^-$ $CD3^-$ $HLADR^+$ $CD16^{+/-}$ $CD14^{+/-}$) were isolated from healthy volunteers. One million of each APC population was live labelled with TelC-probe and stimulated with ionomycin. EVs were analyzed using a Cytoflex LX (Beckman Coulter).

DNA content of telomere vesicles by qPCR

Telomere vesicles were purified by fluorescence activated vesicle sorting and analysed by qPCR (Absolute human telomere length quantification qPCR Assay kit"; ScienCell-Research Laboratories 8918). $CD4^+$ T cells nuclear extracts served as positive control for non-telomeric amplification. In protection assays, telomere vesicles derived from ionomycin activated were treated with the endonuclease DNase I (Benzonase nuclease 70664, 10U, 45min) to digest DNA, in the presence or in the absence of 1% Triton X-100 followed by qPCR with telomere specific primers. For inactivation of DNAase I prior to PCR amplification, samples were heated at 100°C for 5 min.

Telomeric and non telomeric DNA content of released vesicles by slot blot

APC supernatants were treated with DNAse 10 U, 45min (Benzonase® Nuclease, 70664) to digest DNA out of vesicles. DNA vesicles were then purified with Purelink genomic DNA Mini kit (K1820-02). DNA was denatured with NaOH based-denaturing buffer (100 mM NaOH, 10 mM EDTA) at 95°C for 10min. Stop reaction with 20X SSC on ice for 2 mins up to 2XSSC. DNA was then spotted on nylon membrane under vacuum with TelC and Alu probes (Bioptica; Cat. T-1053-400, 1:10000 from stock). Signals were detected with DIG-TelC-probe and DIG-Alu probe following according to TeloTAGGG™ Telomere Length Assay Roche (12209136001).

Dot blot analysis of telomere vesicles

APCs were labelled with BrdU as above described, then cultured with T cells or activated with ionomycin for 18h. Supernatants were then collected from cultures, purified by sequential centrifugation, and DNA secreted by APCs was firstly concentrated 60 min at -80 °C by adding Ethanol/sodium acetate, then immunoprecipitated with anti-BrdU (Abcam AB6326, 0,025µg/µl) in the presence of 1% Triton-X100 (Sigma-aldrich, 9036-19-5) at 4°C. The next day, BrdU immunoprecipitates were incubated with Agarose A/G beads (1:100; Santa Cruz Biotechnology) and kept rotating at 4°C for 3h. Beads were washed twice with ice-cold HNGT buffer (50 mM HEPES, pH 7.5, 150 mM EDTA, 10 mM sodium pyrophosphate, 100 mM sodium orthovanadate, 100 mM sodium fluoride, 10 mg/ml aprotinin, 10 mg/ml leupeptin, and 1 mM phenylmethylsulfonyl fluoride) and once with TE buffer. Beads were then incubated in elution buffer (1% SDS in TE buffer) for 15 min at 65 °C. Telomere vesicles were then eluted by centrifuging at 15,871g for 30 min and dot blotted on Amersham Hybond-N+ nylon membrane (GE, Cat. RPN119B). The membrane

Europe PMC Funders Author Manuscripts

was denaturated in 0.5 M NaOH, 1.5 M NaCl, neutralized and UV-cross linked for 2 min. Telomere dot blot was performed by 3h hybridization at 42°C with DIG-labelled telomere probe as recommended by the manufacturer (Telo-TAGGG Telomere Length Kit Assay; Roche). Input was 200 ng genomic APC DNA. Presence of single strand versus double strand telomeric DNA was confirmed by 10mM EDTA plus 100mM NaOH denaturation followed by 10min at 95°C prior to transfer onto Nylon membranes. For detection of nontelomeric DNA, vesicles were analysed by slot blot with DIG-Alu DNA ctrl probe (Bioptica T-1053-400).

Protein cargo of telomere vesicles

Protein cargo was analysed by indirect ELISA after overnight incubation of vesicle extracts (obtained by 1% Triton x-100) onto binding plates with a final volume of 50µl. After overnight incubation, plates were washed 3 times in 0.1% Tween-20 in TBS and incubated overnight at 4C with antibodies to: MHC II (Abcam ab55152), TZAP (Abnova H00003104-B01P), CD63 (GeneTex GTX28219), BRCA2 (Abcam ab123491), TSG101 (GeneTex GTX70255), Rad51(Abcam ab63801). All antibodies were used at 1:100 dilution. Background control plates were incubated with PBS. Antibody specificity was confirmed by staining parallel vesicle extracts with IgG (isotype control Cell Signaling, 3900S). Primary antibodies were then detected using horseradish peroxidase (HRP) conjugated antibodies (anti-mouse or anti-rabbit IgG, 31430 or 31460 both from Invitrogen) at 1:1,000 dilution in 5% non-fat dry milk 0.1% Tween-20 in TBS, at room temperature for 2h. After washing secondary antibodies 3 times in 0.1% Tween-20 in TBS, 50 µl TMB substrate (N301, ThermoScientific) was added in each well to detect signals for 15 min followed by 50µl stop solution (N600, ThermoScientific). Absorbance was detected at 450nm with an Elisa micro-plate reader (Agilent BioTek AMR-100).

Telomere restriction fragment (TRF) analysis

Autologous APCs and primary human T cells ($5x10^6$) were conjugated 1:1 with for 24h in the presence of antigen pool described above. The day after, conjugates were broken using a 2-ml syringe with cold PBS plus 5mM EDTA and T cell and APC fractions purified by CD3 Microbeads described above. In parallel, identical numbers of T cells and APCs were left unconjugated for comparison of telomere length before and after forming the synapse. Total genomic DNA was used as loading control and detected by anti-dsDNA antibodies (1:10000; Abcam ab27156). Genomic DNA extracted using the PureLink™ Genomic DNA Mini Kit (K182001, ThermoScientific). Telomere length was analysed following the TeloTAGGG™ Telomere Length Assay (12209136001, Sigma-Aldrich).

For TRF on APC vesicle preparations, 1.5 µg of vesicle DNA (recovered after final 100,000g ultra-centrifugation of APC supernatants) were analysed in the presence or in the absence of HinF I/Rsa I (10729124001 Sigma-Aldrich; ER0801 Thermo-Fisher) restriction enzymes to digest non-telomeric DNA (1,5U, 60 min at 37°C).

Telomere Length Quantification Assay

Genomic DNA extraction from T cells and APCs isolated from conjugates was performed according to PureLink Genomic DNA Mini Kit protocol (Invitrogen). qPCR reaction was

performed in the extracted DNA according to the protocol suggested by the “Absolute human telomere length quantification qPCR Assay kit” (ScienCell-Research Laboratories 8918). Telomere length was calculated from the ΔCT, according to the formula suggested by the kit mentioned above.

Universal-STELA

Briefly, 10 ng of MseI and NdeI digested DNA derived from $CD3^+$ $CD4^+$ $CD27^+$ $CD28^+$ T cells was incubated with 12-mer and 42mer panhandles at 65 °C then cooled to 16°C in 49 minutes. T4 DNA ligase was then added to the mixture overnight and kept at 16°C (final volume, 15 µl). The digested DNA was then incubated with 10-3 µM terminal adapters (telorettes) in a final volume of 25 µl and incubated overnight at 35°C. Next, a PCR reaction was set using 40 pg of ligated DNA, in the presence of 0.1 µM adapter and teltail primers and using failsafe master mix and failsafe enzyme. The PCR conditions were as follows: 1 cycle at 68°C for 5 min; 1 cycle at 95°C for 2 min; 26 cycles at 95°C for 15 sec; 26 cycles at 58°C for 30 sec; 26 cycles at 72°C for 12 min; 1 cycle at 72°C for 15 min. The PCR product was then resolved as per TRF analysis on a 0.8% Agarose gel and the load of ultra-short telomeres was calculated as number of telomere bands <3kb/ genome equivalent as described[48]. U-STELA PCR primers (5’—3’) are listed in Supplementary table 3.

Analysis of telomere single-stranded DNA (ssDNA) by qPCR

Briefly, DNA was amplified by two PCR rounds (2xPCR). In the first round, 4 ng of DNA was added to a 25 µl of a master mix comprising (final concentration in parentheses): water, 5X Colorless GoTaq® Reaction Buffer (1×), dNTPs (250 µM), telomere primer set (0,25 µl) and GoTaq® G2 DNA Polymerase (0.025 U/µl) and the samples subjected to: 2 cycles; 40°C for 5 min ramp to 72°C, at 2°C per min, and 10 min 72°C. PCR products were purified (QIAquick PCR Purification Kit, 28104, Qiagen) and subjected to a second qPCR round using the Absolute Human Telomere Length Quantification qPCR Assay Kit (8918, Sciencell). Vesicle DNA (4 ng) was also analysed by single round qPCR (1xPCR) using the same kit. Percentage of ssDNA was calculated as: ssDNA(%) = kb (2xPCR)- kb (1xPCR) *100% / kb (1xPCR)

Flow-FISH

For determination of absolute telomere length (kb) by Flow-FISH, we used a previously generated standard curve formed by cryopreserved samples with known telomere length as examined by Southern blot of telomeric restriction factors (TRFs). This standard curve allows conversions of Flow-FISH MFI values into TRF kb by calculating Molecules of Equivalent Soluble Fluorochrome (MESF) units[4]. Immune conjugates were analyzed over a 48h time course using.

Generation of T cell chromosomes with APC telomeres

For EdU labelling, APCs were separately activated with GMCSF (10ng/ml; GF304 Merck) and IL-4 (50ng/ml; 130-093-922 Miltenyi) for 48h in the presence of 10 µM EdU (Click-iT™ EdU Cell Proliferation Kit for Imaging, Alexa Fluor™ 488 dye; C10337 Thermofisher), with no contact with T cells. T cells were separately activated (48h) with

Europe PMC Funders Author Manuscripts

anti-CD3 plus anti-CD28 antibodies (0.5 μg/mL each) and treated with 3,000 TelC-Cy5$^+$ Edu-labelled telomere vesicles derived after FAVS from supernatants of EdU-labelled, ionomycin-activated APCs. The T cells were then treated with colcemid (0.2 μg/mL; 15212012 Life technologies) in the last 4 hours of activation, to derive metaphase spreads. For metaphase spreads generation, T cell metaphase spreads were swollen 5 min in KCl buffer (12.3 mM HEPES, 0.53 mM EGTA, 64.4 mM KCl), fixed 5 min in methanol: glacial acetic (3:1 solution) then dried 60 min onto pre-warmed glass-slides. T cell chromosomes with APC telomeres were analysed by Edu reaction chemistry and telomeres and colocalization with Edu telomere from vesicles and standard telomere FISH with Cy-3, and TelC/EdU colocalisation events enumerated. For metaphase Q-FISH, T cell chromosomes with APC-telomeres were generated as above described in the absence of any standard telomere FISH, and directly quantified by Q-FISH coupled to TFL software analysis (TeloV2) in parallel with internal standards with known telomere length.

For mouse experiments, APCs were *in vivo* labelled by IP injection with 100 μl of 1 mg/ml EdU in PBS. Mice were then administered 0.3 mg/ml EdU in drinking water *ad libitum* for 14 days. Water was replaced with fresh Edu every 2 days. The Edu-labelled APCs were then loaded with OVA antigen (3 μM) and conjugated with OT-II CD4+ T cells from congenic mice not labelled with EdU for 24 hours. Colcemid (0.2 μg/mL; 15212012 Life technologies) was added for 4h before conjugates being disrupted through a 2-ml syringe, and the OT-II CD4$^+$ T cells fraction isolated by mouse anti-CD3. The post-synaptic telomere acquiring OT-II CD4$^+$ T cells were then spun 300g on image coverslips ready for IF-FISH.

APC-T cell telomere fusion

T cells (10^6) were cultured for 48h with 5,000 telomere vesicles or 5,000 telomere depleted vesicles. In some experiments, blocking antibodies to MHC class II (1μg/mL; ab55152 Abcam) were added to the vesicle preparations prior to transfer into T cells, as indicated. T cell nuclear extracts were derived using nuclear extract lysis buffer from Pierce™ Chromatin Prep Modulen 26158) then analysed by qPCR using telomere specific and standard primers (8918, ScienceCell research Laboratories) using standard 6800 Roche Analyzer.

In vivo Telomere Transfer

C57BL/6J mice and OT-II mice (C57BL/6-Tg(TcraTcrb)425Cbn/Crl) were purchased from Charles River. TelC-Cy3-probe labelled mouse APCs were loaded with 3 μM OVA peptide (GeneScript 323-339) and injected into the right footpad of wild type C57BL/6J recipients. The day after, OVA-specific OT II cells (identified by Cell Trace Violet dye staining) were adoptively transferred. Popliteal lymph nodes were harvested after additional 18h and APC->T cell telomere transfer examined by flow cytometry. In control experiments, APCs were not loaded with OVA antigens. For CTV staining, the manufactures instruction were followed (CellTrace™ Violet Cell Proliferation Kit, for flow cytometry; C34557). APC TelC labelling of terminal donor T cell chromosomes after *in vivo* telomere transfer was generated upon treatment with colcemid but in the absence of any standard FISH. Donor OT-II CD4+ T cells were transferred as per CTV experiments but using GFP$^+$ T cells instead to allow tracking in recipients. GFP$^+$ T cells were obtained by *in vitro* transduction with GFP mock pDual vectors (11155 Addgene) 10 days prior to injection.

Memory/Effector responses

Naïve CD45.2 $CD4^+$ OTII $CD4^+$ T cells were isolated from OT-II mice (C57BL/6-Tg(TcraTcrb)425Cbn/Cr; Charles River) using mouse Naïve $CD4^+$ T cells isolation kit (Miltenyi 130-104-452). Naïve CD45.2 OTII CD4+ T cells were then coupled with congenic mouse CD45.2 APCs (CD3-depleted splenocytes, by CD3e Microbeads kit mouse Miltenyi 130-094-973) that were previously live-labelled with Cy3 TelC probes, in the presence of OVA antigen (3μM). Twenty-four hours later, the $CD3^+$ $CD4^+$ OTII were sorted based on APC-derived TelCy3 telomere fluorescence, into Tel^+ (that acquired telomeres from APCs) vs Tel^- (that did not acquire telomeres in the same synaptic process). One thousand CD45.2 OT-II $CD4^+$ T cells were injected[49] into wild type C57BL/6 CD45.1 recipient mouse followed by OVA vaccination (30mg) 18 eighteen hours later. For effector responses, CD45.2 OTII $CD4^+$ T cells were analysed 5 days after the first *in vivo* OVA vaccination from the blood, spleen and lymph nodes of CD45.1 recipients; for memory responses, mice were stimulated with a second round of OVA vaccination (30μg) 40 days post transfer, rested for 50 days and memory responses assessed 90 days after adoptive transfer. CD45.2 CD4+ OTII T cells were enriched from blood, lymph nodes and spleen by using 2ug/ml CD45.2-biotin antibody (130-124-089, Miltenyi) and pulled down with 50 ul of Streptavidin Microbeads (130-048-101, Miltenyi). Total mouse CD4+T cells (including both recipient CD45.1 CD4+ T cells and donor CD45.2 CD4+ T cells) from recipient mice were stained with anti-CD4 (Miltenyi 130118955) anti-CD44 (Miltenyi, Cat. 130119121), anti-CD62L (Miltenyi 130112649), anti-CD45.1 (Miltenyi 130121221), anti-CD45.2 (Milteny 130124 080), and anti-CD95 (Miltenyi 130122950). All antibodies were used at 1:100 dilution.

Recombinogenic potential of Rad51 telomere vesicles *in vivo*

CD45.2 $CD4^+$ OTII T cells were isolated from C57BL/6-Tg (TcraTcrb)425Cbn/Cr; Charles River) with mouse CD4 microbeads (L3T4 Microbeads 130-117-043; Miltenyi). The T cells were then treated with 500 siCtrl or siRad51 telomere vesicles derived upon FAVS purification of supernatants from siCtrl or siRad51 transfected APCs, labeled with PKH67 and TelC probes (as above) and stimulated with ionomycin. For siCtrl transfection, (sc-37007); for siRad51 (sc-36360), both from Santa-Cruz Biotechnology. Vesicle treated CD45.2 $CD4^+$ OTII T cells ($5x10^5$) were then intravenously injected into CD45.1 recipients. Eighteen hours later, mice were vaccinated with 30μg OVA peptide (323-339; GeneScript). Forty days later, mice were revaccinated with OVA (second round *in vivo*) then culled after an additional 30-day observation (a 70 day experiment). Telomere depleted vesicles served as control. CD45.2 $CD4^+$ OTII T cells from lymph nodes and spleen were examined by flow cytometry.

Survival studies

C57BL/6J mice were vaccinated with FLUAD (1:20 of the human dose; Sequirus) and after five days, sacrificed, spleens collected and total $CD4^+$ T cells were isolated as above. Total $CD4^+$ T cells were incubated with vesicles containing telomeres (Tel+ ves) or depleted of telomeres (Tel- vesicles) (5000 vesicles per $5x10^6$ T cells per recipient mouse) and then injected in each recipient C57BL/6J mice by caudal intravenous injection. Ctrl group was injected with $CD4^+$ T cells not primed with the vaccine. Mice were early

(after 18 hours) or delayed (after 15 days) challenged with H1N1 flu virus ($3,5*10^5$ PFU; VR-1469 ATCC). H1N1 flu viral particles were diluted in 40 ul of PBS (per mouse) and intra-nasally administered. Survival was monitored for 15 days and clinical score was recorded throughout. Mice were sacrificed when a clinical score was equal or above 10, or in any case severe dyspnoea was observed. Clinical scoring for sign of illness (Supplementary table 4) was adapted[50] under veterinary assessment and according to ethical approval.

Measurement of Telomerase activity

Telomerase activity was assessed with a TeloTAGGG telomerase ELISA kit according to the manufacturer's instructions (Roche) and extracts of 2×10^3 viable $CD3^+$ $CD4^+$ $CD27^+$ $CD28^+$ T cells as described previously[14].

Long-term cultures

Primary human $CD3^+$ $CD4^+$ $CD27^+$ $CD28^+$ T cells were activated by anti-CD3/anti-CD28 antibodies (0.5 μg/mL each) every 10 days in the presence or absence of telomere vesicles or telomere depleted vesicles as control and their population doublings calculated as described previously[14].

Immunological analysis by flow-cytometry

Primary human $CD3^+$ $CD4^+$ $CD27^+$ $CD28^+$ T cells (10^5) were activated with anti-CD3 (0.5 μg/mL) and recombinant human (rh) IL-2 (10ng/ml) for 10 days in the presence of 250-1,000 telomere vesicles (purified from either human or mouse CD3-depleted APC preparations as indicated), telomere depleted vesicles or left without any vesicle. Ten days later, the T cells were analysed on a Beckman Coulter flow cytometry with multiparametric settings. For the immunophenotype characterization, T cells were stained with anti-CD4 Alexa 700 (clone OKT4, Biolegend, Cat. 317626, 1:100), anti-CD27 PerCP5.5 (clone M-T271, Biolegend, Cat. 356408, 1:100), anti-CD28 APCVio770 (clone REA612, Miltenyi Biotec, Cat. 130-116-506, 1:100), anti-CD45RA BV421 (clone HI100, Biolegend, Cat. 3104130, 1:100), anti-CD45RO ECD (clone UCHL1, Beckman Coulter, Cat. M2712U, 1:100), anti-CD75 (Miltenyi Cat. 130113068), anti-PD1 APC (clone NAT105, Biolegend, Cat. 367406, 1:100), antiFasL PE-Cy7 (clone NOK-1, Biolegend, Cat. 306418, 1:100), anti-CTLA4 PE (clone L3D10, Biolegend, Cat. 349906, 1:100) and anti-TIM-3 VioBright FITC (clone REA602, Miltenyi Biotec, Cat. 130-109-711, 1:50). Cells were washed in PBS and analysed on a Cytoflex flow cytometer (Beckman Coulter).

Cell death analysis

APCs were activated with ionomycin (0.5 μg/ml) as above or conjugated with autologous T cells (3:1) in the presence or absence of antigen pool. Cell death was analysed 18h later by FITC Annexin V/PI Apoptosis Detection Kit with PI (640914; Biolegend).

Measurement of senescence-associated-b-galactosidase

Human T cells ($2x\ 10^5$) were activated by anti-CD3 plus anti-CD28 either in the presence or in the absence of 1,000 telomere vesicles from APCs for 10 days. After overnight resting at 37 degrees °C, cells were cytospun 5' at 500 rpm and senescence-associated

beta-galactosidase activity measured as recommended by the manufacturer (Cell Signaling Technology Cat.23833S) on a Zeiss-Axio inverted phase-contrast microscope. Control APCs were activated either in the absence of vesicles or with telomere depleted vesicles or with siRad51 telomere vesicles.

APC-T cell Telomere co-localization

Fluorescent (Cy-3) APC-telomere enriched supernants were added drop by drop into autologous resting primary human T cells that had been previously labelled with FITC (488)-TelC PNA telomere probes and cultured onto poly-lysine-coated coverslips. APC-T cell telomere co-localization into the nuclei of recipient T cells was assessed by ImageJ software. Costes method was used to verify colocalization thresholds against randomly generated images[51]. Co-localization frequencies were calculated within a single stack with the following formula: **Z/(X+Y-Z)*100%** where *Z* is number of co-localization events; *X* is the number of T cell telomeres; and *Y* is the number of transferred telomeres of APC-origin.

Chromatin Immunoprecipitation

Primary human T cells (10^7) were activated overnight by anti-CD3 plus anti-CD28 (both at 0.5 μg/ml) in the presence or absence of Cy3-TelC-labelled APC-derived enriched supernatants containing telomeres derived from ionomycin activated TelCy3 live-labelled APCs. Cells were cross-linked 10 min with 1% formaldehyde, lysed and their nuclei digested with MNase-based Thermofisher Pierce Agarose Chip kit (Pierce™ Chromatin Prep Module, 26158). Digested chromatin was immunoprecipitated with polyclonal anti-POT1 or control rabbit IgG antibodies at 4C on a rotary shaker overnight followed by incubation with Chip-grade A/G agarose beads (sc-500775; Santa Cruz Biotechnology) at 4C for 3 hours. Presence of APC-derived telomeres in control and POT-1 (1:100; PA-66996, ThermoFisher) immunoprecipitated T-cell reactions was quantified as Cy3 absorbance emission of triplicate wells using a micro-plate reader. Presence of APC-derived telomeres was further confirmed by adding DNAse directly to the POT1 IPs for 10 min prior to reading. Background fluorescence was calculated in parallel POT1 immunoprecipitation reactions from activated $CD3^+$ $CD4^+$ $CD27^+$ $CD28^+$ T cells not treated with APC-derived telomeres.

Supported planar bilayers

Glass coverslips were cleaned 20 min with Piranha solution, rinsed extensively and dried. Coverslips were plasma cleaned 4 min then assembled into ibidi chambers for bilayer formation. Lipid bilayers containing 12.5% mol NTA (1,2dioleoyl-*sn*-glycero-3-*N*-5-amino-1-carboxypentyl iminodiacetic acid succinyl) and and 0.004% CapBio (1,2-dioleoyl-*sn*-glycero-3-phosphoethanolamine-*N*-cap biotinyl) in DOPC (1,2-dioleoyl-*sn*-glycero-3-phosphocholine) were incubated 20 min at a total phospholipid concentration of 0.4 mM. After washing in 0.1% HBS/BSA, bilayers were blocked 20 min with 2% BSA/HBS containing 100 μM NiSO4, washed extensively, and loaded 20 min with 4μg/mL streptavidin. Streptavidin-coated bilayers were subsequently coated 20 min with 1.1 μg/ml UCHT1 568 (anti-CD3 or anti-TCR; final density: 30 molecules/ μm^2) and 0.39 μg/ml ICAM-1 405 (anti-LFA1; final density: 200 molecules/ mm^2). Bilayers were washed and

immediately used for synapse formation. $CD3^+$ $CD4^+$ $CD27^+$ $CD28^+$ T cells were activated on bilayers for 20 min, fixed 10 min with 2% PFA then imaged in TIRF mode with Olympus 150x 1.45 NA objective. Primary human T cells were loaded onto bilayers directly *ex vivo* or after overnight resting in complete RPMI at 37°C.

Extraction of APC-telomeres on planar bilayers

Planar bilayers were constructed as above described and incubated with primary human $CD3^+$ $CD4^+$ $CD27^+$ $CD28^+$ T cells. After 20 min activation on bilayers, $CD3^+$ $CD4^+$ $CD27^+$ $CD28^+$ T cells were removed with cold PBS. The released synaptic TCRs were retained on the bilayer, as described[19]. Next, telomere-live-labelled APCs (obtained by introducing and TelC probe by glass beads as above described) were loaded with antigen pool and transferred on the TCR coated planar bilayers. The % of APCs releasing telomeres on bilayers was quantified 24h later. In control experiments, APCs were not loaded with antigen pool; or they were transferred onto bilayers constructed with ICAM-1 molecules alone without UCTH1. The vesicular nature of the released telomeres was further tested by pre-incubating TelC labelled APCs with antibodies to the vesicle marker CD63 (clone H5c6; Biolegend Cat. 353015) at 1:50 dilution prior to transfer on bilayer.

Field Emission Scanning Electron Microscopy

Samples (APCs or telomere vesicles purified by fluorescence-activated vesicle sorting), were adhered on Ply-L-Lysine-coated round glass coverslips of 1 cm diameter, then fixed with 2.5% glutaraldehyde in 0.1M sodium cacodylate buffer (pH 7.4) at room temperature for 1h. Fixed samples were rinsed 10 minutes with 0.1M sodium cacodylate buffer (3 times), then dehydrated through ethanol gradients (30%, 50%, 70%, 85%, 95%, 100% - 10 mins at room temperature for each ethanol concentration). A 1:1 ethanol: hexamethyldisilazane (HMDS) mix was then added to the samples for 5 min at room temperature followed by a final 5 min step incubation in HMDS. All samples were then left drying overnight. The upper base of each aluminium stub was coated with colloidal silver paint and the coverslips were pasted onto them. Samples mounted on stubs were coated with a gold layer by Q150R S Rotary-Pumped Sputter Coater (Quorum Technologies) and examined by FESEM (Sigma-Zeiss) at an accelerating voltage of 2 kV using secondary electron (SE) detection. A number of regions of interest (ROIs) containing single or multiple APCs for each sample were recorded to confirm absence of glass beads or to depict structural alterations. Micrographs of telomere vesicles were used to perform particle size distribution analysis by measuring the diameter of each adhered telomere vesicle.

Immunogold analysis of telomere vesicles

Human APCs (10^8) were live-labelled with TelC-biotinylated PNA probes as above described, then stimulated with ionomycin for 18h. The 10,000g ultracentrifuged supernatants (1mL) were then loaded over 100 ul of 30% sucrose solution in PBS without mixing the two layers, and ultracentrifuged at 100,000g for 90 minutes at 4 °C using SorvallTM WX 90+ ultracentrifuge (Thermo Fisher Scientific). The supernatants were then discarded and the sucrose layer (~200 ul) washed with 1 ml ice-cold PBS followed by further ultracentrifugation at 100,000g for 90 minutes. Vesicle pellets were resuspended in 40 μL fixing solution (2% paraformaldehyde, 0.125% glutaraldehyde in 0.1 M sodium

phosphate buffer), then fixed for 1h at 4°C on a rocker. 5-μl of vesicle preparations were mounted on Formvar/Carbon 200 Mesh Cu grids (Agar Scientific Ltd), and the grids left to air dry for 10 min. Vesicles were permeabilized with 0.1 % saponin diluted in PBS for 30 min, and washed twice in PBS. Samples were incubated in blocking buffer (1% Bovine Serum Albumin (BSA), 20 mM glycine in PBS) for 45 min, then labelled with Strepavidin-collodial 10 nm gold conjugate (S9059, Sigma Aldrich; 1:10 dilution) in blocking/permeabilizing buffer at 4 °C for 1h on a rocker. The vesicles were washed 6 times in blocking buffer (1:10 in PBS) followed by incubation in 1% (v/v) glutaraldehyde for 5 min and washed in ddH2O. Grids were negatively stained using 1% phosphotungstic acid (Electron Microscopy Sciences) for 1 min and the excess removed using a filter paper. Finally, the grids were air dried for 10 min and examined on a Philips EM 208S (FEI) transmission electron microscope with an accelerating voltage of 80 kV. Images were captured on a MegaView III (Olympus Soft Imaging Solutions).

Exclusion of APC-telomeres in T cell plasma membranes

Primary human T cells were activated by anti-CD3 plus anti-CD28 for 24h in the presence of Cy3 labelled APC telomere vesicles, T cell plasma membranes were then purified with Plasma Membrane Protein Extraction Kit (ab65400; Abcam) and absence APC telomeres assessed by confocal imaging on Leica SP2. Plasma membrane purification was confirmed by CellMask dye (C10046; Invitrogen).

Statistical analysis

All human and mouse experiments were performed with at least three independent biological samples, up to nine different donors or mice, as indicated. GraphPad Prism v9 was used to perform statistical analysis. For pairwise comparisons in human experiments, a two-tailed, paired Student's t-test was used. For pairwise comparison in *in vivo* mouse experiments, a two-tailed, unpaired Student's t-test was used. For multiple comparisons, a one-way analysis of variance (ANOVA) for repeated measures with a Bonferroni post-test correction was used. For synapse studies with two samples, Mann-Whitney test; for those with three or more synapse groups, Kruskal-Wallis. For survival analysis, Mantel-Cox. For co-localization studies, Pearson's or Mander's co-localization tests, as indicated. Exact p-values are shown in each figure panel. Ns, (not significant) >0.5 are provided within Source data.

Europe PMC Funders Author Manuscripts

Europe PMC Funders Author Manuscripts

Extended Data

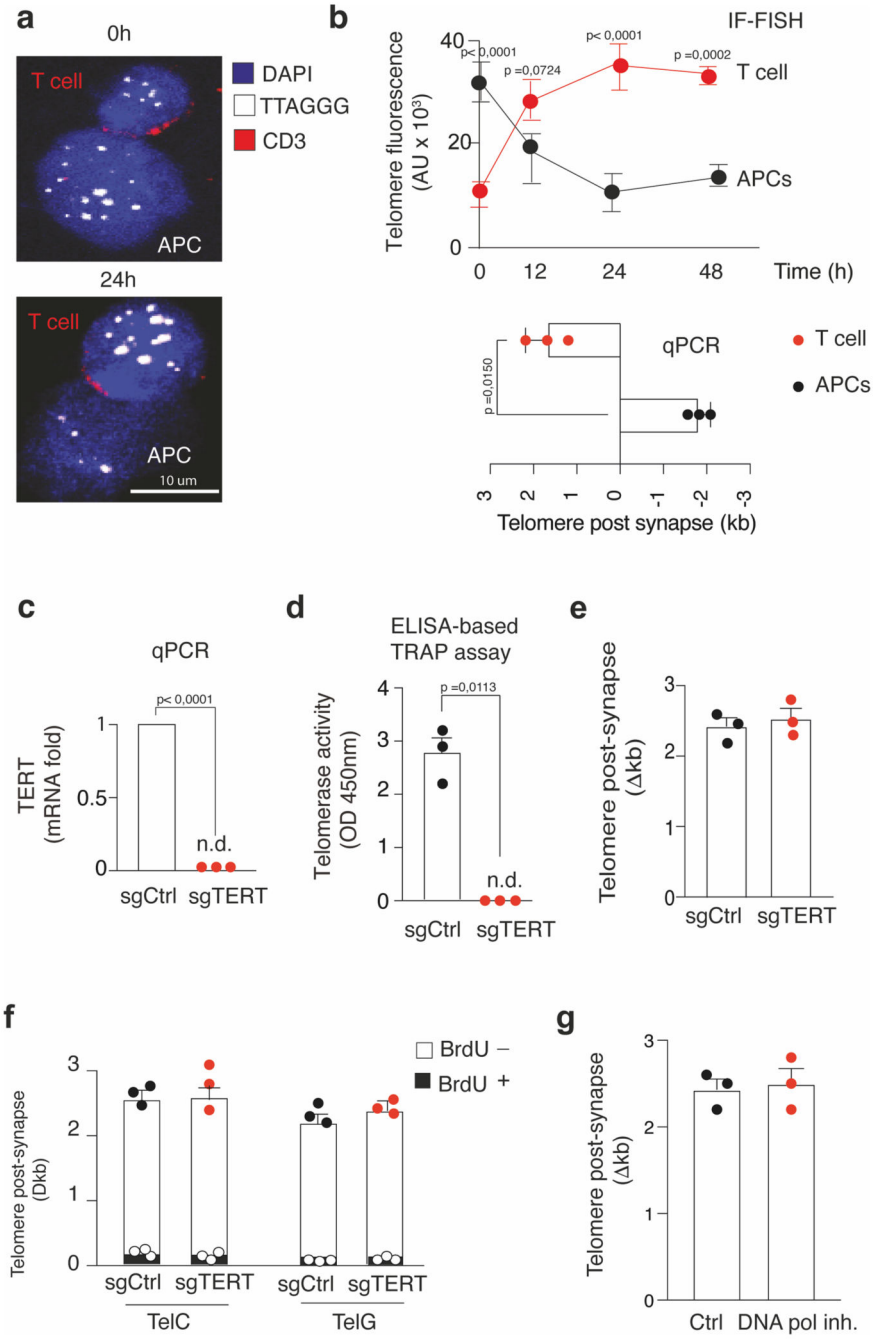

Extended Data Fig. 1. Telomere elongation in the absence of DNA synthesis

(**a**) Representative IF-FISH and (**b, top**) pooled data showing telomere elongation in nonsenescent CD4+ T cells and concomitant telomere shortening in APCs after forming the synapse. APCs from human donors were pre-loaded with cytomegalovirus lysates and allowed to interact with autologous nonsenescent $CD4^+$ T cells in 3:1 ratio for the indicated time points. Conjugates were fixed and analysed by IF-FISH. Data are from n=3 donors

Europe PMC Funders Author Manuscripts

(three independent experiments). Scale bar, 10 μm. T=0, initial time at which conjugates are observed (20 min). Images were z-stacked, and the raw telomere integrated fluorescence signals (AU, arbitrary units) are shown. One-hundred two conjugates were analysed. (**b, bottom**) Analysis of telomere length by qPCR in APCs and nonsenescent CD4+ T cells after forming conjugates. (**c-d**) Primary human nonsenescent $CD4^+$ T cells were transfected by nucleofection with sgCtrl or sgTERT CRISPR constructs, activated with anti-CD3 plus anti-CD28 and elimination of telomerase was confirmed by (**c**) qPCR and (**d**) TRAP assay. (**e**) Telomerase positive (transfected with sgCTRL) and negative (transfected with sgTERT) nonsenescent T cells were exposed to APCs in the presence of antigen pool, and telomere content was quantified by Flow-FISH using TelC telomere probe. Absolute telomere length by Flow-FISH was determined from Mean Fluorescence Intensity (MFI) values using a standard curve formed by cryopreserved samples with known telomere length as determined by TRF. (**f**) Telomere content was measured by flow-FISH using either TelC or TelG telomere PNA specific probes coupled to anti-BrdU detection (to monitor telomere elongation *vs* DNA synthesis in T cells) in telomerase negative nonsenescent $CD4^+$ T cells (CRISPR KO sgTERT) and control T cells (sgCtrl) stimulated with antigen pool for 48h. (**g**) Telomere length by flow-FISH demonstrating telomere elongation in primary human nonsenescent $CD4^+$ T cells treated with DNA polymerase inhibitors aphidicolin and thymidine prior to exposure to APCs for 48h. Data are from n=3 donors throughout. Statistical Tests are provided in the Supplementary Table 1. Error bars indicate S.E.M. throughout.

Europe PMC Funders Author Manuscripts

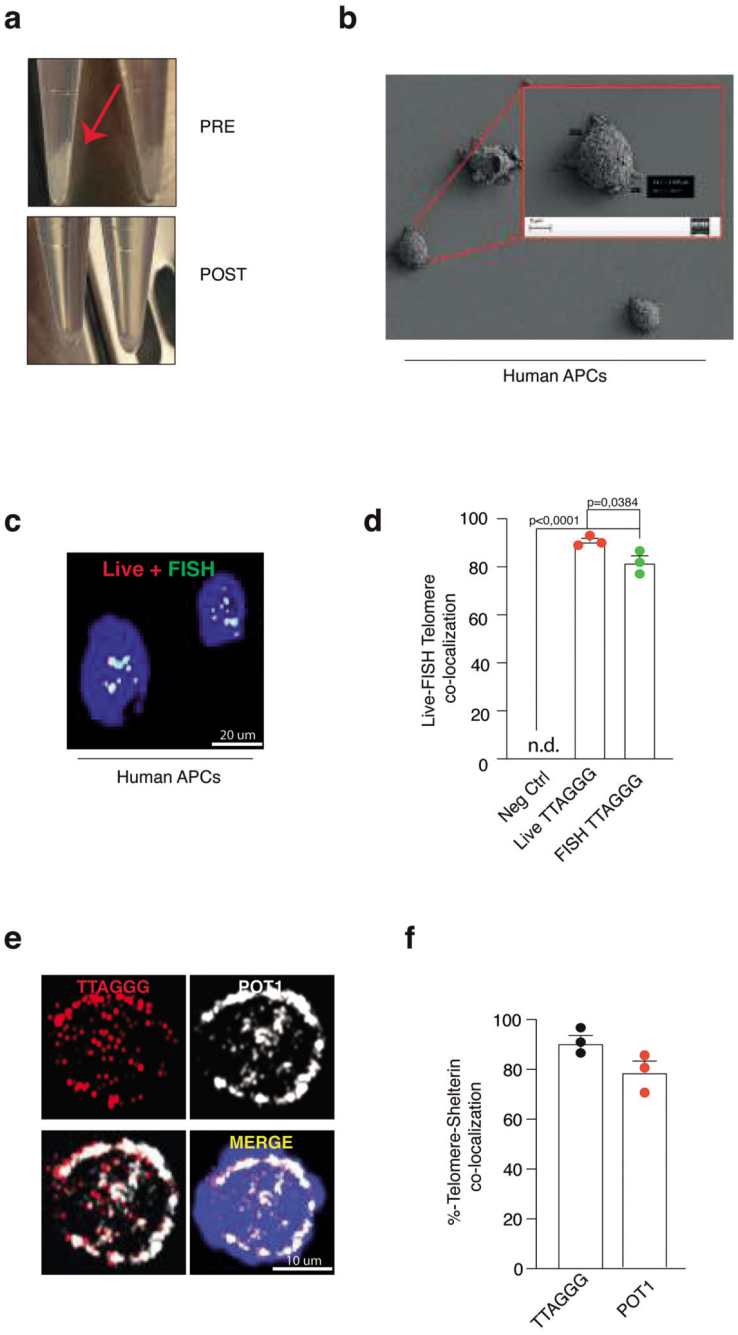

Extended Data Fig. 2. Generation of live APCs with fluorescent telomeres

(**a**) PNA-telomere probes were dissolved 1:50 in telomere loading buffer (80 mM KCl, 10 mM K2PO4, 4 mM NaCl, pH 7.2) and gently introduced on adherent APCs by rolling large glass beads (size: 400-600 mm) for 2 min on cell surface to create temporary pores on the APC membranes and allow telomere TelC PNA probe entry into the APCs while preserving their viability (no cell fixative) needed for subsequent synapse studies with T cells. Arrow indicates beads. The beads were completely removed by washing two times with PBS prior to assays. (**b**) Absence of any residual glass beads from TelC PNA probe labelled

APCs was confirmed by FESEM. Scale bar, 2 μm. Representative of n=3 experiments (three donors). (**c**) Identical telomere detection by FISH (fixed cells) or glass bead-mediated telomere PNA probe delivery (live cells) in APCs. Nuclei were counterstained by DAPI (blue). Representative of n=4 experiments (four donors). Scale bar, 20 μm. (**d**) Manders colocalization scores of experiments as in (**c**). Negative control, APCs with unlabelled telomeres. (**e**) Immunofluorescence staining of POT1 and telomere TelC PNA probe live delivery on primary human APCs (CD3-depleted PBMCs). POT1 recruitment to telomeres was detected directly *ex vivo*. Scale bar, 10 μm. (**f**) Manders co-localization scores of experiments as in (**e**). Results are from n=3 donors (two experiments). Statistical Tests are provided in the Supplementary Table 1. Error bars indicate S.E.M. throughout..

Europe PMC Funders Author Manuscripts

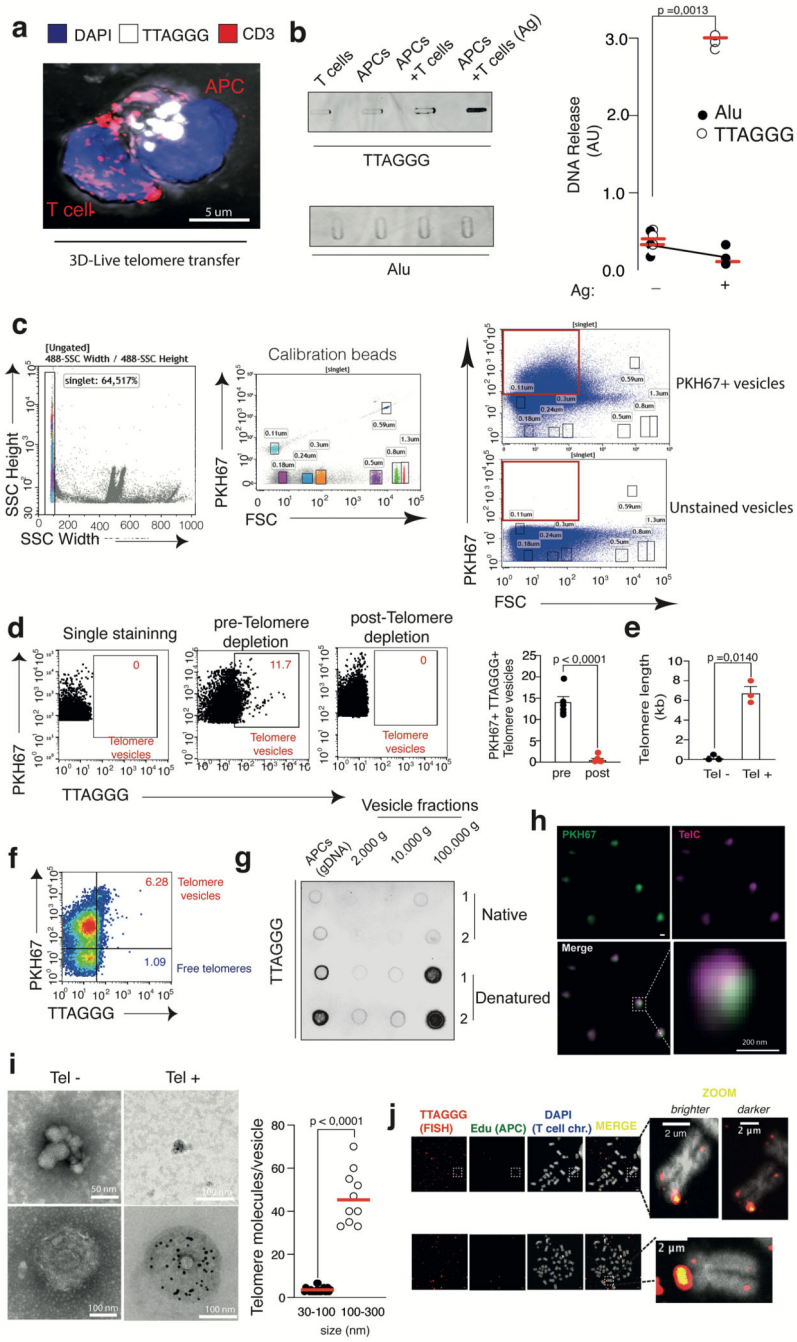

Extended Data Fig. 3. APCs donate telomere vesicles

(**a**) Telomere transfer through the immune synapse, confocal imaging. Scale bar, 5 µm. Representative of n=3 donors. (**b, top left**) Telomere vesicle release triggered by 18h antigen-specific contacts of APCs and nonsenescent $CD4^+$ T cells. (**b, bottom left**) Alu release in the same T cells. (n=6 donors **b, right**). (**c, left and middle**) Side scatter (SSC) threshold and calibration beads used in FAVS-based vesicle purifications, gated on singlets (Extended Data Fig. 3c, **left panel**). Extended Data Fig. 3c, **middle panel**, size of the beads. (**c, right**) PKH67 lipid staining of all vesicles produced by primary human APCs

upon 18h ionomycin activation. Unstained PKH67, threshold control. Gating strategy for individual vesicles <100 nm up to 300 nm. Larger particles (>300 nm) due to aggregates were excluded. (**d, left**) PKH67 staining and (**d, middle and right**) presence of telomere vesicles in ~10% of the total APC single particle vesicle fraction. (*n*=9 donors; **d, far right**). (**e**) Telomeric DNA from telomere vesicles was purified and confirmed by qPCR (*n*=3 donors form three independent experiments). (**f**) Presence of a small population (~1%) of vesicle free telomeres released by APCs during FAVS. Representative of *n*=9 experiments. (**g**) Dot-blot analysis of telomeric DNA isolated from different fraction of vesicles isolated from sequential centrifugation of APC supernatants under native or denaturing conditions. APC genomic DNA (gDNA), loading control. Representative of *n*=3 donors. (**h**) Super-resolution Zeiss Airyscan microscopy of FAVS-purified Tel^+ vesicles. A representative experiment from *n*=3 independent experiments (three donors) is shown. Scale bar, 200 nm. (**i**) TEM analysis of Tel-vs Tel+ vesicles. Examples for small-sized vesicles (**top**) and larger vesicles (**bottom**) are shown for both Tel^- and Tel^+. Quantifications of telomeric DNA in telomere vesicles distributed by size (**right**). Representative images (**left**) and pooled vesicle data (**right**) (*n*=10; from three independent experiments).(**j**) Further examples of T cell chromosomes with APC telomeres. Metaphase experiments of T cells with APC telomeres were performed *n*=5 times. Statistical Tests are provided in the Supplementary Table 1. Error bars indicate S.E.M. throughout.

Europe PMC Funders Author Manuscripts

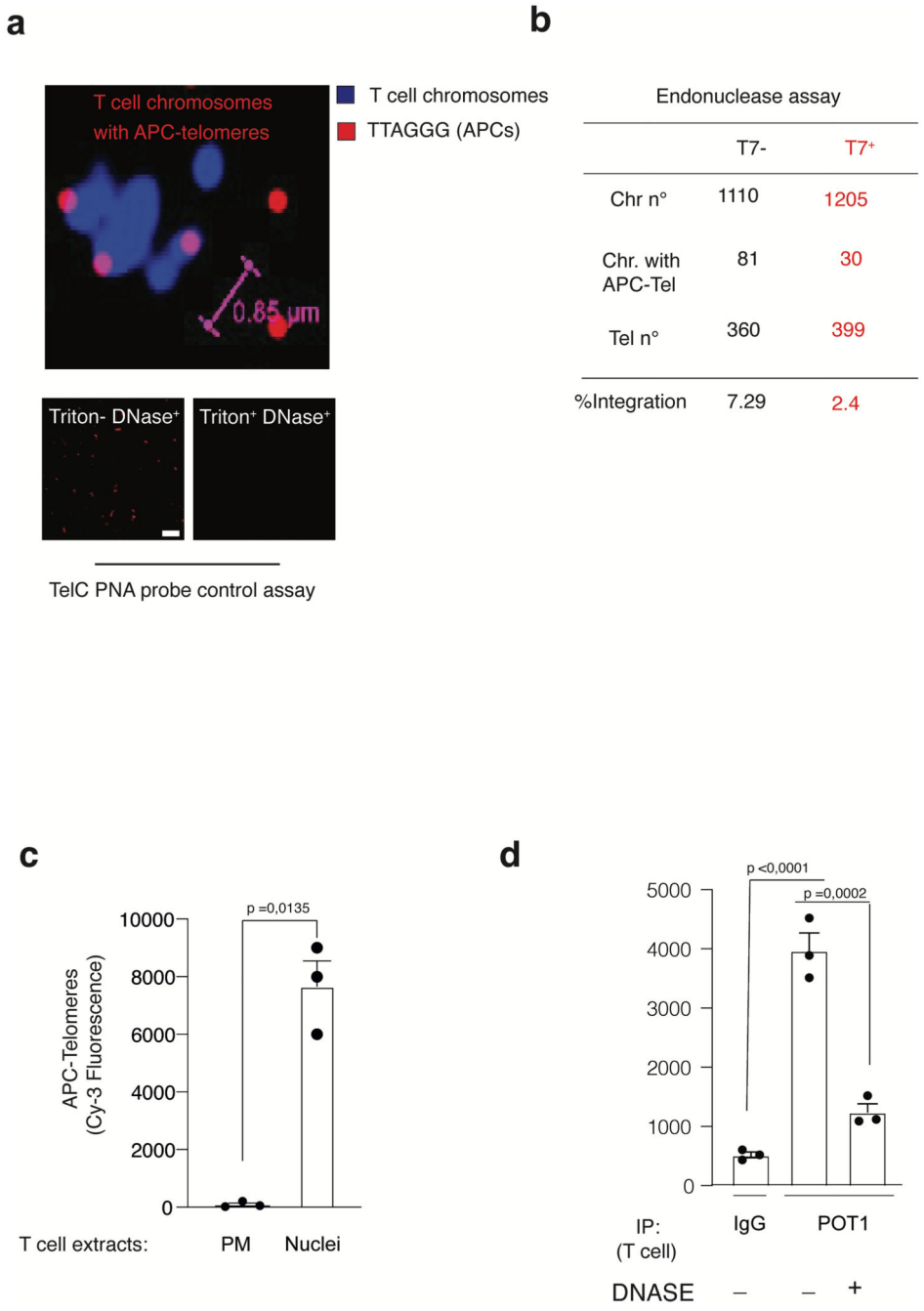

Extended Data Fig. 4. APC telomeres at T cell chromosome ends

(**a**) Representative metaphase spreads showing T cell chromosomes with APC derived telomeres. Scale bar, 0.85 µm. Representative of *n*=3 donors. (**b**) Metaphase spreads generated as in (**a**) were treated with 1 unit T7 endonuclease for 30 min at 37 °C. The number of T cell chromosomes with APC telomeres before (black values) and after (red values) T7 endonuclease treatment is shown. Pooled from *n*=3 experiments (three donors). (**c**) Presence of APC-derived telomeres in purified nonsenescent T cell plasma membranes from (10^6) *vs* T cell nuclei from the same cells 24h after transfer of fluorescent telomere

Europe PMC Funders Author Manuscripts

enriched supernatants derived from APCs activated with ionomycin. The T cell plasma membranes were assessed by confocal imagining on LEICA SP2. APC telomeres were only observed in the nuclear fraction but not in the T cell plasma membrane after the 24 hours incubation. Pooled data from n=3 independent experiments (three donors). (**d**) Quantification of APC telomere signal after T cell chromatin immunoprecipitation. Primary human nonsenescent $CD3^+$ T cells (10^7) were activated by anti-CD3 plus anti-CD28 overnight in in the presence or absence of fluorescent telomere enriched supernatants. The nuclei were digested after lysis with MNase-based Thermofisher Pierce Agarose Chip kit. Chromatin derived from digestion was immunoprecipitated with polyclonal anti-POT1 (1:100) or control rabbit IgG antibodies. The Cy3-fluorescence of APC-derived telomeres was quantified with a microplate reader. Control IP, T cell extracts precipitated with irrelevant IgG. Presence of APC-derived telomeres was confirmed by adding DNase directly to the POT1 IP for 10 min at room temperature prior to fluorescence reading. Pooled results from n=3 donors. Statistical Tests are provided in the Supplementary Table 1. Error bars indicate S.E.M. throughout.

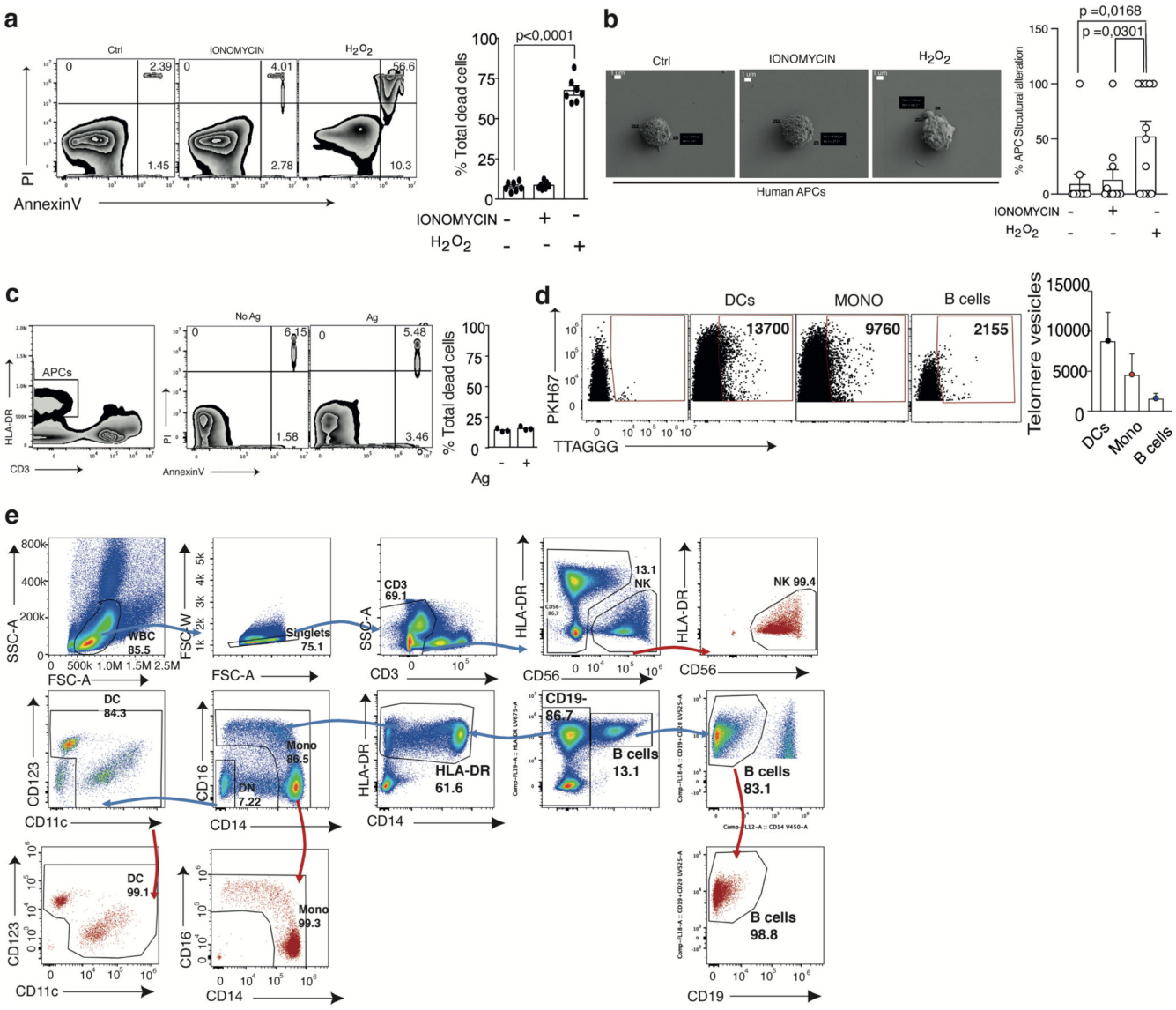

Extended Data Fig. 5. Telomere transfer does not cause APC death

(**a**) Analysis of cell death of APCs after 18h stimulation with or without ionomycin (0.5 mg/mL), or with hydrogen peroxide (H2O2; 500 mM) as death positive control. Cell death was analysed 18h later by FITC Annexin V/PI Apoptosis staining with flow cytometry. Pooled data from n=7 independent biological experiments are shown. **(b)** FESEM micrographs (10,000x) of resting APCs or activated APCs upon treatment with ionomycin or H2O2 for 18h. Scale bar 1μm. Pooled data from n=12 micrographs (3-5 APCs per micrograph at 10,000x magnification) depicting %APCs with structural alterations (blebbing or membrane damage) are shown. Note that ionomycin treatment does not induce membrane blebbing. APCs treated with H2O2 (500μM) served as positive control throughout experiments. Each dot is an individual cell from n=3 independent experiments (three donors) (**c, left**). APCs were coupled to nonsenescent $CD4^+$ T cells in the presence or in the absence of the antigen pool for 18h then analysed by Annexin/PI with flow cytometry. (**c, right**). Pooled results

Europe PMC Funders Author Manuscripts

from n=3 independent experiments (three donors). (**d**) APCs were separated into their main subsets of DCs, Monocytes and B cells by FACS sorting then 10^6 cells/subset were live labelled with TelC PNA probes and PKH67 lipid dye, stimulated with ionomycin for 18h, followed by FAVS analysis of APC subset supernatants. Note that hypo or non-proliferative myeloid cells are the major telomere donors. (**d, right**) Cumulative data from n=3-4 donors are shown (three experiments). (**e**) The sorting strategies and related purities to derive DCs (99.1%), Monocytes (99.3) and B cells (98.8%) for experiments in (**d**). Statistical Tests are provided in the Supplementary Table 1. Error bars indicate S.E.M. throughout.

Europe PMC Funders Author Manuscripts

Europe PMC Funders Author Manuscripts

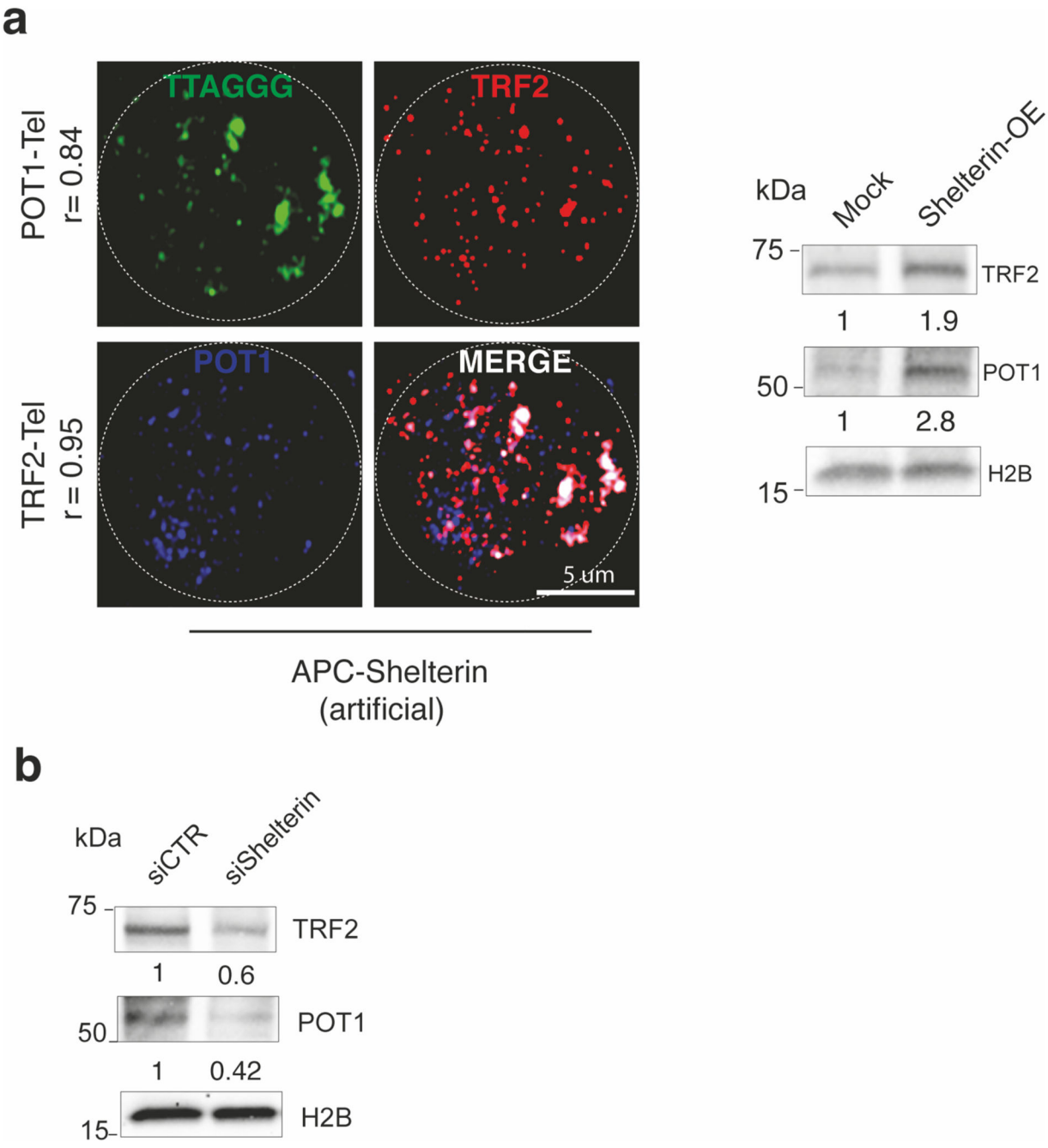

Extended Data Fig. 6. Generation of artificial shelterin APCs

(**a, left**) IF-FISH demonstrating recruitment of artificial shelterin factors (POT1 and TRF2) to telomeres in primary human APCs transduced with the lentiviral vectors (mock vector and TRF2/POT1 vectors, see methods) and activated with ionomycin for 18h, 96h post transduction. The Pearson's co-localization score for artificial POT1 and TRF2 with APC telomeres are shown. Scale bar, 5 μm. (**a, right**) Validation of shelterin overexpression (TRF2 and POT1) by immunoblotting in primary human APCs. Numbers indicate shelterin overexpression efficiency. H2B, loading control. (**b**) Immunoblot analysis of TRF2 and

POT1 following indicated siRNA treatment in primary human APCs. H2B, loading control. The numbers indicate knock-down efficiency. Shelterin knock down APCs were generated by siTRF2 plus siPOT1 transfection from resting primary human APCs. Seventy-two hours later telomere release was analyzed as above described in the absence of ionomycin activation. Results are representative of n=3 independent experiments (three donors) throughout.

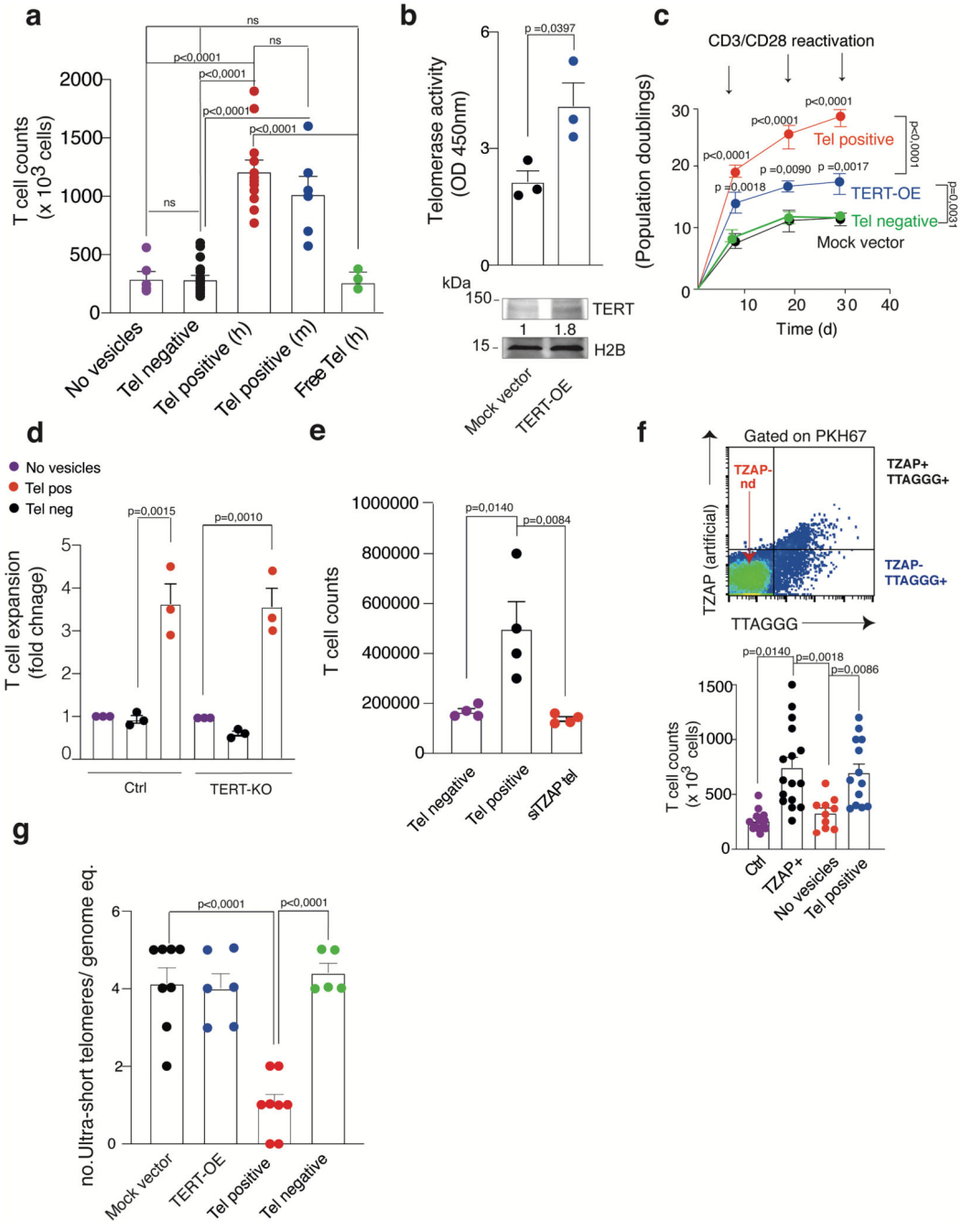

Extended Data Fig. 7. Telomere vesicle effects do not require telomerase.

Europe PMC Funders Author Manuscripts

(**a**) Expansion of human T cells by heterologous telomere vesicles. Nonsenescent $CD4^+$ T cells were activated with anti-CD3 and anti-CD28 and cultured ten days with or without 1,000 telomere vesicles (Tel^+) or telomere depleted vesicles (Tel^-) purified by FAVS. The vesicles were derived from donor mismatched human (h) or mouse (m) APCs, as indicated, upon ionomycin activation. Different biological cultures are shown (n= 6 no vesicle; n= 18 Tel neg; n= 12 Tel pos human, n= 6 Tel pos; n= 3 free Tel human). (**b**) Confirmation of CRISPR-based telomerase enhancement in nonsenescent $CD4^+$ T cells by TRAP assay (**top**) and immunoblots (**bottom**). (**c**) Population doublings (n = 3 donors) of nonsenescent $CD4^+$ T cells cultured as indicated for 30 days. **(d)** Telomere positive and negative nonsenescent $CD4^+$ T cells were activated with anti-CD3 and anti-CD28 for 10 days in the presence of 1,000 telomere vesicles, telomere depleted vesicles or left without any vesicles; n=3 experiments (three donors) throughout cultures. (**e**) Defective proliferation in primary human nonsenescent $CD4^+$ T cells supplemented with siTZAP telomere vesicles that do not express TZAP compared to those expressing TZAP. Results from n=4 independent experiments (four donors). (**f, top**). Telomere vesicles produced by TZAP-artificial APCs were purified by FAVS following ionomycin activation for subsequent stimulation of T cells. (**f, bottom**) Proliferative expansion of T cells with TZAP+ vesicles was tested as in (**a**). N= 13 (Ctrl); n= 16 (TZAP+), n= 10 (no vesicle); n= 14 (Tel pos). **(g)** Reduced load of ultra-short telomeres (<3kb) in nonsenescent $CD4^+$ T cells activated by anti-CD3 plus anti-CD28 for 48h followed by transfer of 1,000 FAVS-purified telomere vesicles (Tel pos) or vector-based telomerase enhancement assessed by U-STELA. Controls, T cells with mock vector or 1,000 telomere depleted vesicles. Results from n=5 (tel neg); n= 8 (tel pos; mock vector) or n= 6 (TERT-OE). Statistical Tests are provided in the Supplementary Table 1. Error bars indicate S.E.M. throughout..

Europe PMC Funders Author Manuscripts

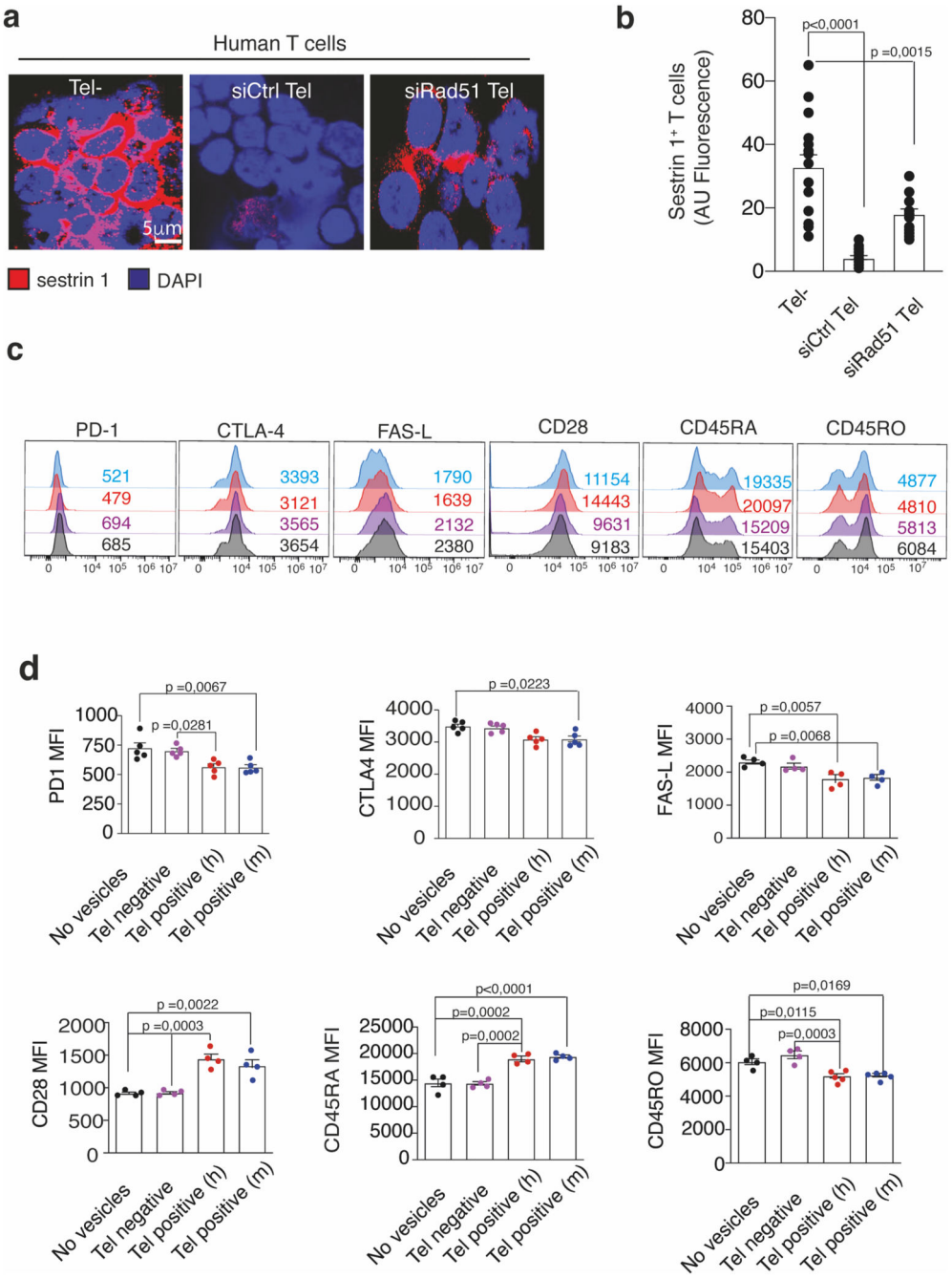

Extended Data Fig. 8. Signaling and phenotypic changes of T cells with APC telomeres

(**a**) Representative immunofluorescence (IF) staining of sestrin 1 in primary human T cells cultured with or without telomere vesicles derived from APCs previously transfected with either siCtrl or siRad51 RNAs then transferred to primary human nonsenescent $CD4^+$ T cells activated by anti-CD3 plus anti-CD28 for ten days. Telomere depleted vesicles (telomere neg) as background control. Representative of 3 donors. (**b**) Data shown are pooled from n=3 donors, with each dot being an individual T cell. (**c**) Primary human nonsenescent CD4+ T cells (10^5) were activated with anti-CD3 (0.5 mg/mL) and recombinant human

Europe PMC Funders Author Manuscripts

IL-2 (10ng/mL) for 10 days in the presence of 250 FAVS-purified telomere vesicles derived from either human or mouse APCs prior to multiparametric flow cytometry. Control T cells were activated without any vesicle or with 250 telomere depleted vesicles obtained by FAVS. Representative plots and (**d**) pooled data from *n*=5 independent experiments are shown. Numbers indicate mean fluorescence intensity (MFI) value from a representative experiment. Statistical Tests are provided in the Supplementary Table 1. Error bars indicate S.E.M. throughout.

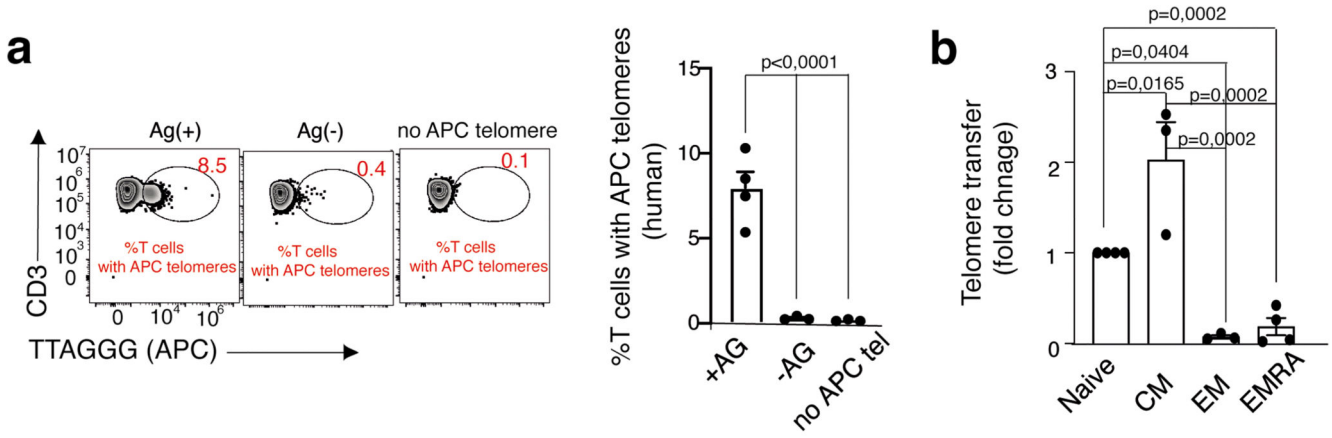

Extended Data Fig. 9. Naive and central memory T cells are the major telomere acquiring cells from APCs.

(**a**) Analysis of telomere transfer by flow FISH flow cytometry upon conjugation of APCs live-labelled with TelC PNA telomere probes and total primary human $CD3^+$ T cells for 24 hours. Each dot is an individual donor from $n = 4$ independent biological experiments. Control, APCs loaded with antigen pool and stimulated with T cells but without telomere labelling throughout experiments (no APC telomere). No antigen (pool) control is also shown confirming antigen dependency. (**b**) Naïve and central memory T cells are the major APC telomere acquiring cells. Purified primary human $CD4^+$ T cell populations ($CD28^+$ $CD45RA^+$ naïve purity 98.7%; $CD28^+$ $CD45RA^-$ central memory (CM) purity 95%; $CD28^-$ $CD45RA^-$ senescent effector memory (EM) 97.5%; senescent $CD28^-$ $CD45RA^+$ EMRA purity 94%) were treated as in (**a**) and telomere transferred was measured by flow FISH with TelC probe. Pooled results from $n = 3$ (CM and EM) and $n = 4$ (naïve and EMRA) independent individual donors. Note that since primary human $CD4^+$ T cells first lose expression of CD27 followed by that of CD28, $CD28^-$ $CD4^+$ T cells are highly differentiated cells, many of which are considered senescent[8,31–34,45]. The opposite regulation occurs in primary human CD8 T cells, where the $CD27^-$ population is considered highly differentiated/senescent since the cells first expression of CD28 followed by that of CD27[9,32]. The reason for this is not known. Statistical Tests are provided in the Supplementary Table 1. Error bars indicate S.E.M.

Europe PMC Funders Author Manuscripts

Europe PMC Funders Author Manuscripts

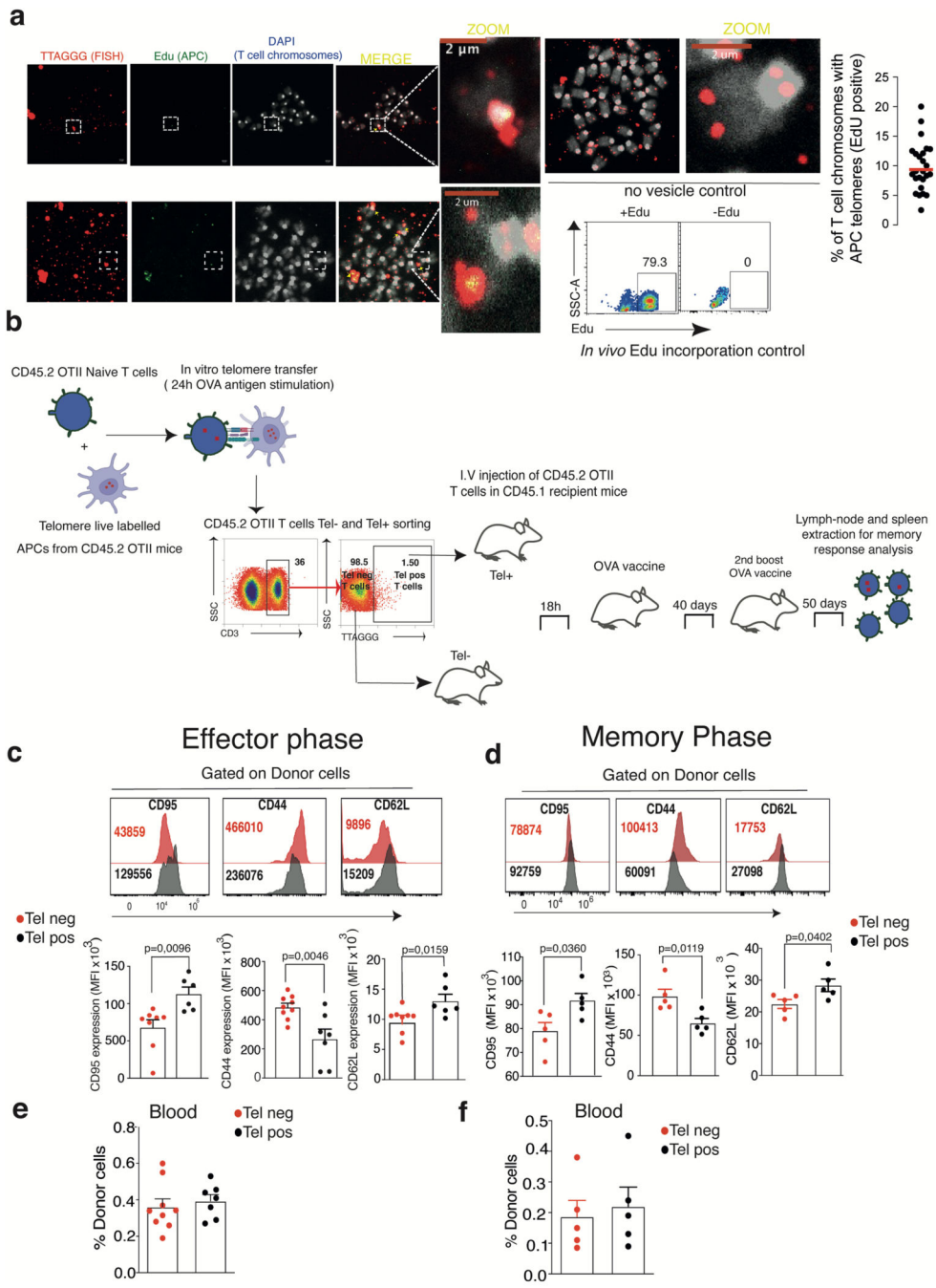

Extended Data Fig. 10. Existence of T cells with telomeres of APC origin in mice

(**a**) Quantification of APC telomeres at mouse T cell chromosomes upon *in vivo* APC labelling. Two representative examples are shown. As control, mouse OTII CD4$^+$ T cells were analysed by IF-FISH in the absence of telomere vesicles (no vesicle control). Scale bar, 2µm. FACS plot, Edu incorporation control in donor APC prior to telomere transfer. Representative of n=3 mice. (**b**) Naïve CD45.2 OTII CD4$^+$ T cells were incubated with congenic TelC labelled APCs in the presence of OVA (3 µM) for 18 hours then sorted into CD45.2 OTII CD4$^+$ Tel+ (T cells with APC telomeres) versus CD45.2 OTII CD4$^+$

Tel- (T cells without APC telomeres) based on telomere transfer prior to transfer into CD45.1 recipients and vaccination with OVA (30 μg). Effector responses were assessed 5 days post-transfer; for memory responses mice were re-vaccinated with OVA (30 μg) forty days after the first vaccination and observed after additional fifty days. Note that the *in vitro* efficacy of telomere transfer is much lower than that observed *in vivo*, possibly due to the well-recognized lower efficiency of *in vitro* APC-T cell conjugates versus their physiological counterparts *in vivo*. (**c**) Phenotype of donors CD45.2 OTII $CD4^+$ T cells as in Fig. 6h. and (**d**) the same markers for experiments as in Fig. 6i-j. (**e-f**) Percentage of CD45.2 OTII $CD4^+$ Tel+ *vs* CD45.2 OTII $CD4^+$ Tel- in the blood of recipient mice vaccinated with OVA during effector and memory responses. Each dot is an individual animal (Tel neg *n*= 9; Tel pos n=7 animals, **e**; and n = 5 per group in **f**). Statistical Tests are provided in the Supplementary Table 1. Each dot is an individual mouse. Error bars indicate SEM.

Supplementary Material

Refer to Web version on PubMed Central for supplementary material.

Acknowledgements

This study was supported by the Wellcome Trust (110229/Z/15/Z) and the Italian Ministry of Health (GR-2018 12365916) to A.L. Laboratory infrastructures were provided by Sentcell ltd. M.L.D. was supported by the Wellcome Trust Principal Research Fellowship 100262Z/12/Z and the Kennedy Trust for Rheumatology Research. A.N.A. was supported by the Medical Research Council (MR/P00184X/1). M.K. is supported by the NIH (R37AI04477). A.L. is an Honorary Associate Professor of the University College London and the Chief Executive Officer of Sentcell ltd. The funders had no role in study design, data collection and analysis, decision to publish or preparation of the manuscript.

Data availability

Source data are provided with this paper. Further data supporting the findings of this study are available from the corresponding author upon reasonable request.

References

1. Kipling D. Telomeres, replicative senescence and human ageing. Maturitas. 2001; 38: 25–37. [PubMed: 11311583]
2. Hayflick L, Moorhead PS. The serial cultivation of human diploid cell strains. Exp Cell Res. 1961; 25: 585–621. [PubMed: 13905658]
3. Blasco MA. Telomeres and human disease: ageing, cancer and beyond. Nat Rev Genet. 2005; 6: 611–22. [PubMed: 16136653]
4. Collins K. Mammalian telomeres and telomerase. Current Opinion in Cell Biology. 2000; 12: 378–383. DOI: 10.1016/S0955-0674(00)00103-4 [PubMed: 10801465]
5. Cesare AJ, Reddel RR. Alternative lengthening of telomeres: models, mechanisms and implications. Nature Reviews Genetics. 2010; 11: 319–330.
6. Fooksman DR, et al. Functional anatomy of T cell activation and synapse formation. Annual Review of Immunology. 2010; 28: 79–105.
7. Akbar AN, Beverley PCL, Salmon M. Will telomere erosion lead to a loss of T-cell memory? Nat Rev Immunol. 2004; 4: 737–43. [PubMed: 15343372]
8. Weng N-P, Akbar AN, Goronzy J. CD28(-) T cells: their role in the age-associated decline of immune function. Trends Immunol. 2009; 30: 306–12. [PubMed: 19540809]

9. Plunkett FJ, et al. The Loss of Telomerase Activity in Highly Differentiated CD8+CD28-CD27-T Cells Is Associated with Decreased Akt (Ser473) Phosphorylation. The Journal of Immunology. 2007; 178: 7710–7719. [PubMed: 17548608]
10. Boraschi D, et al. The gracefully aging immune system. Sci Transl Med. 2013; 5 185ps8
11. Goronzy JJ, Weyand CM. Understanding immunosenescence to improve responses to vaccines. Nat Immunol. 2013; 14: 428–36. [PubMed: 23598398]
12. Lanna A, et al. A sestrin-dependent Erk-Jnk-p38 MAPK activation complex inhibits immunity during aging. Nature Immunology. 2017; 18
13. Akbar AN, et al. Senescence of T Lymphocytes: Implications for Enhancing Human Immunity. Trends in Immunology. 2016; 37: 866–876. [PubMed: 27720177]
14. Lanna A, Henson SM, Escors D, Akbar AN. The kinase p38 activated by the metabolic regulator AMPK and scaffold TAB1 drives the senescence of human T cells. Nat Immunol. 2014. 1–10.
15. Akbar AN, Vukmanovic-Stejic M. Telomerase in T lymphocytes: use it and lose it? J Immunol. 2007; 178: 6689–94. [PubMed: 17513711]
16. Hodes RJ, Hathcock KS, Weng N. Telomeres in T and B cells. Nat Rev Immunol. 2002; 2: 699–706. [PubMed: 12209138]
17. Dustin ML, Groves JT. Receptor signaling clusters in the immune synapse. Annu Rev Biophys. 2012; 41: 543–56. [PubMed: 22404679]
18. Chakraborty AK, Weiss A. Insights into the initiation of TCR signaling. Nature Immunology. 2014; 15: 798–807. [PubMed: 25137454]
19. Choudhuri K, et al. Polarized release of T-cell-receptor-enriched microvesicles at the immunological synapse. Nature. 2014; 507: 118–123. [PubMed: 24487619]
20. Molenaar C, et al. Visualizing telomere dynamics in living mammalian cells using PNA probes. EMBO J. 2003; 22: 6631–41. [PubMed: 14657034]
21. Messenger SW, Woo SS, Sun Z, Martin TFJ. A Ca2+-stimulated exosome release pathway in cancer cells is regulated by Munc13-4. Journal of Cell Biology. 2018; 217: 2877–2890. [PubMed: 29930202]
22. van der Vlist EJ, Nolte-'t Hoen ENM, Stoorvogel W, Arkesteijn GJA, Wauben MHM. Fluorescent labeling of nano-sized vesicles released by cells and subsequent quantitative and qualitative analysis by high-resolution flow cytometry. Nat Protoc. 2012; 7: 1311–1326. [PubMed: 22722367]
23. Hadden JM, Déclais A-C, Carr SB, Lilley DMJ, Phillips SEV. The structural basis of Holliday junction resolution by T7 endonuclease I. Nature. 2007; 449: 621–624. [PubMed: 17873858]
24. Li JSZ, et al. TZAP: A telomere-associated protein involved in telomere length control. Science. 2017; 355: 638–641. [PubMed: 28082411]
25. Denchi EL, de Lange T. Protection of telomeres through independent control of ATM and ATR by TRF2 and POT1. Nature. 2007; 448: 1068–1071. [PubMed: 17687332]
26. Sfeir A, de Lange T. Removal of Shelterin Reveals the Telomere End-Protection Problem. Science (1979). 2012; 336: 593–597.
27. Park JY, Jang SY, Shin YK, Suh DJ, Park HT. Calcium-dependent proteasome activation is required for axonal neurofilament degradation. Neural Regen Res. 2013; 8: 3401–9. [PubMed: 25206662]
28. Tarsounas M, et al. Telomere maintenance requires the RAD51D recombination/repair protein. Cell. 2004; 117: 337–47. [PubMed: 15109494]
29. Vallejo AN, Brandes JC, Weyand CM, Goronzy JJ. Modulation of CD28 expression: distinct regulatory pathways during activation and replicative senescence. J Immunol. 1999; 162: 6572–9. [PubMed: 10352273]
30. Warrington KJ, Vallejo AN, Weyand CM, Goronzy JJ. CD28 loss in senescent CD4+ T cells: Reversal by interleukin-12 stimulation. Blood. 2003; 101: 3543–3549. [PubMed: 12506015]
31. Larbi A, Fulop T. From "truly naïve" to "exhausted senescent" T cells: When markers predict functionality. Cytometry Part A. 2014; 85: 25–35.
32. Akbar AN, Fletcher JM. Memory T cell homeostasis and senescence during aging. Curr Opin Immunol. 2005; 17: 480–5. [PubMed: 16098721]

33. Fletcher JM, et al. Cytomegalovirus-Specific CD4+ T Cells in Healthy Carriers Are Continuously Driven to Replicative Exhaustion. The Journal of Immunology. 2005; 175: 8218–8225. [PubMed: 16339561]
34. Gattinoni L, et al. A human memory T cell subset with stem cell-like properties. Nature Medicine. 2011; 17: 1290–1297.
35. Shimatani K, Nakashima Y, Hattori M, Hamazaki Y, Minato N. PD-1+ memory phenotype CD4+ T cells expressing C/EBPα underlie T cell immunodepression in senescence and leukemia. Proc Natl Acad Sci U S A. 2009; 106: 15807–15812. [PubMed: 19805226]
36. Shirakawa K, et al. Obesity accelerates T cell senescence in murine visceral adipose tissue. Journal of Clinical Investigation. 2016; 126: 4626–4639. [PubMed: 27820698]
37. Pearce EL, Poffenberger MC, Chang C-H, Jones RG. Fueling immunity: insights into metabolism and lymphocyte function. Science. 2013; 342 1242454 [PubMed: 24115444]
38. Chang JT, et al. Asymmetric T lymphocyte division in the initiation of adaptive immune responses. Science (1979). 2007; 315: 1687–1691.
39. Gattinoni L, et al. A human memory T cell subset with stem cell-like properties. Nature Medicine. 2011; 17: 1290–1297.
40. Kaech SM, Wherry EJ. Heterogeneity and Cell-Fate Decisions in Effector and Memory CD8+ T Cell Differentiation during Viral Infection. Immunity. 2007; 27: 393–405. [PubMed: 17892848]
41. Chang JT, et al. Asymmetric T lymphocyte division in the initiation of adaptive immune responses. Science (1979). 2007; 315: 1687–1691.
42. Bannard O, Kraman M, Fearon DT. The Secondary Replicative Function of CD8+ T Cells That Expressed Granzyme B During a Primary Anti-Viral Response. Science (1979). 2009; 323: 505–509.
43. Boraschi D, et al. The gracefully aging immune system. Sci Transl Med. 2013; 5 185ps8
44. Di Mitri D, et al. Reversible senescence in human CD4+CD45RA+CD27-memory T cells. J Immunol. 2011; 187: 2093–100. [PubMed: 21788446]
45. Vallejo AN, Schirmer M, Weyand CM, Goronzy JJ. Clonality and Longevity of CD4 + CD28 null T Cells Are Associated with Defects in Apoptotic Pathways. The Journal of Immunology. 2000; 165: 6301–6307. [PubMed: 11086066]
46. Youngblood B, et al. Effector CD8 T cells dedifferentiate into long-lived memory cells. Nature. 2017; 552: 404–409. [PubMed: 29236683]
47. Wijeyesinghe S, et al. Expansible residence decentralizes immune homeostasis. Nature. 2021; 592: 457–462. [PubMed: 33731934]
48. Serakinci N, Cagsin H, Mavis M. Use of U-STELA for Accurate Measurement of Extremely Short Telomeres. Methods Mol Biol. 2019; 2045: 217–224. [PubMed: 29542055]
49. Moon JJ, et al. Tracking epitope-specific T cells. Nature Protocols. 2009; 4: 565–581. [PubMed: 19373228]
50. Huet O, et al. Ensuring animal welfare while meeting scientific aims using a murine pneumonia model of septic shock. Shock. 2013; 39: 488–494. [PubMed: 23603767]
51. Costes SV, et al. Automatic and Quantitative Measurement of Protein-Protein Colocalization in Live Cells. Biophysical Journal. 2004; 86: 3993–4003. [PubMed: 15189895]

Europe PMC Funders Author Manuscripts

Europe PMC Funders Author Manuscripts

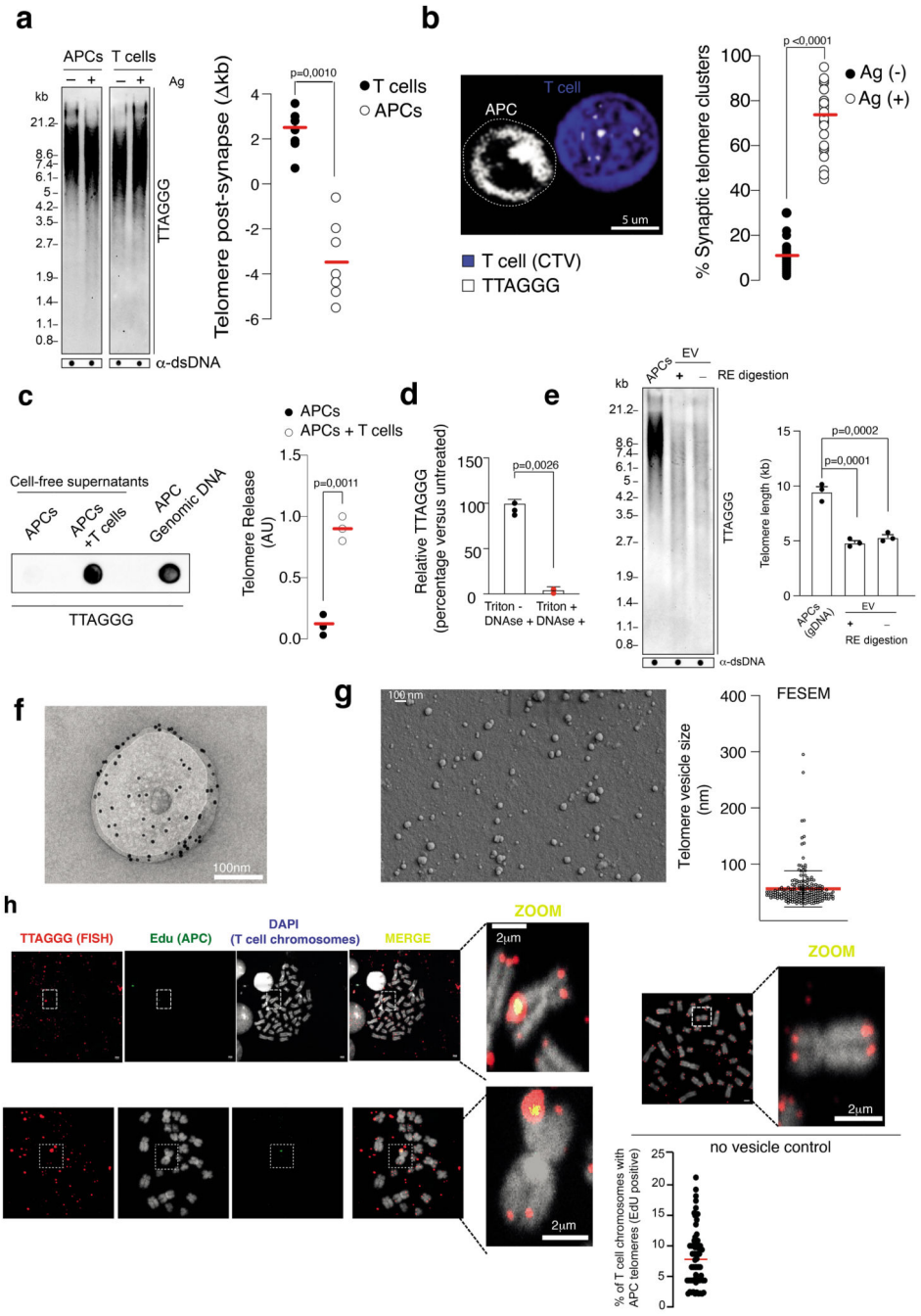

Figure 1. APCs donate telomeres to T cells.

(**a**) TRF analysis of APCs and T cells before and after synapse formation. Loading control, double stranded DNA (dsDNA). Representative (**left**) and pooled data (*n=7* donors) are shown (**right**). (**b**) Telomere clustering in APC-T cell conjugates. Nonsenescent $CD4^+$ T cells were labelled with CTV prior to conjugation with CTV-free APCs for 2h then analysed by Immunofluorescence IF-FISH. Representative conjugate (**left**) and pooled data (**right**) from thirty-seven conjugates (*n*= 3 independent experiments) are shown. Scale bar, 5 μm. (**c**) Telomere donation by APCs upon antigen-specific contact with T cells.

Immunoprecipitates of telomeric DNA donated by BrdU-labelled APCs immunoprecipitated from cell-free supernatants were assessed by dot blot. Input, APC genomic DNA (200 ng). Representative data (**left**) and pooled data (n=3 independent experiments; **right**) are shown. (**d**) DNAse I-based telomere vesicle protection assays by qPCR in the presence or in the absence of 1% Triton-X 100. Pooled data (n= 3 independent experiments) are shown. (**e**) TRF analysis of APC telomeric DNA present in the EVs isolated by ultracentrifugation upon ionomycin activation. Restriction enzyme digestion to remove non telomeric DNA. APC gDNA, positive control. dsDNA, loading controls. Representative data (**left**) and (**right**) pooled data (n= 3 donors) are shown. (**f**) TEM with strepavidin-colloidal 10 nm immunogold conjugate labelling of telomere vesicles released by human APCs. Scale bar, 100nm. A representative telomere vesicle (n= 3 independent experiments) is shown. Additional TEM data, Extended Data Fig. 3i. (**g**) Ultrastructural analysis of telomere vesicles by FESEM following purification by FAVS. Magnification, 100,000X; scale bar, 100nm. Representative images (**left**) and pooled data (**right**) from 204 vesicles are shown (n= 3 independent experiments). (**h**) Detection of T cell chromosomes upon transfer of EdU-labelled APC telomeres by IF-FISH. Representative data (**left** n= 5 donors along with additional examples in ED3j) and their enlargement (**middle**) are shown. Scale bar, 2 μm. Quantification from 2425 chromosomes in the same experiments (**bottom right**). Error bars indicate S.E.M. throughout. Statistical tests, Supplementary table 1.

Europe PMC Funders Author Manuscripts

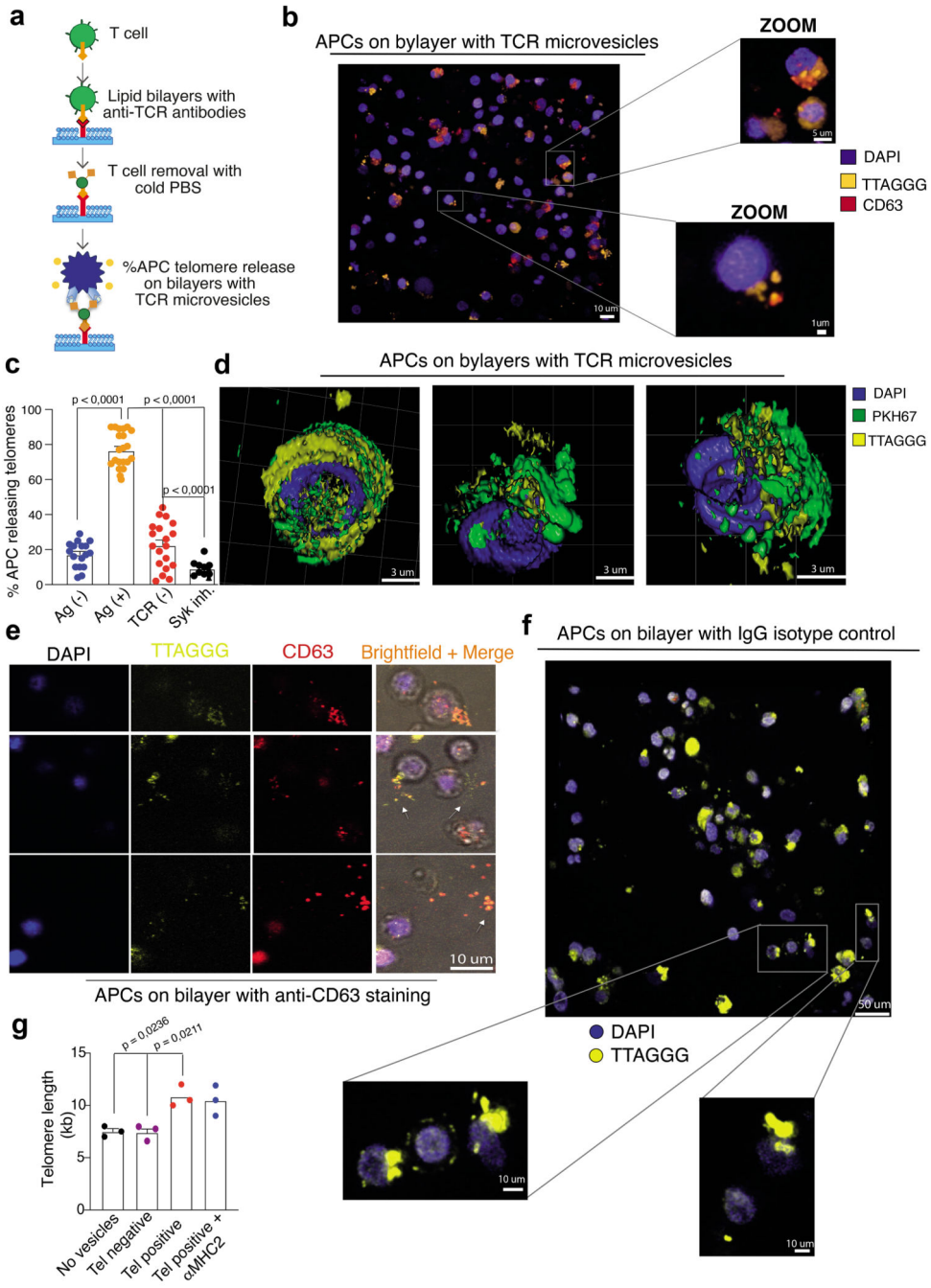

Figure 2. Synaptic TCRs are sufficient to extract telomere vesicles from APCs.

(a) Schematic representation of telomere transfer on artificial synapse bilayers (see Methods). (**b**) Representative release of CD63^{+} telomere vesicles from APCs activated on bilayers. APCs were live-labelled with TelC telomere probes and anti-CD63 prior to transfer on bilayers (n= 3 donors). (**c**) Quantification of antigen-specific telomere release by APCs (n= 4 donors) on bilayers dependent on TCR and antigen availability on the bilayer. Bilayers were either coated with or without anti-TCR followed by loading of nonsenescent CD4^{+} T cells which resulted either in release of TCR (TCR+) or no TCR release on the bilayer

(TCR-) after removal of T cells. TelC-labelled APCs where then either pre-loaded with (Ag+) or without (Ag-) the antigen pool and their telomere release on bilayers quantified. As control, TelC-labelled APCs were pre-treated with Syk inhibitor (Syk inhibitor; 200nM) to inhibit calcium signalling for 30 min in the presence of the antigen pool prior to transfer on TCR coated bilayers. The percentage of telomere releasing APCs was normalized to the total number of APCs on the bilayer. (**d**) Demonstration of lipid content of telomere vesicle released from APCs on planar bilayers (n= 3 donors). Antigen (Ag)-pulsed APCs were live labelled with TelC probes and PKH67 lipid dye then incubated onto bilayers containing synaptic TCRs for 24h. (**e**) Representative release of $CD63^+$ telomere vesicles on planar bilayers documented by brightfield illumination (n= 4 donors). (**f**) Isotype control experiments for telomere vesicle release on bilayers (n= 3 donors). (**g**) Nonsenescent CD4+ T cells (10^6) were cultured for 48 hours with five-thousands telomere vesicles (Tel+) purified from APCs by FAVS, in the presence or absence of blocking MHC II antibodies (1 μg/mL), then analysed by qPCR. Five-thousands telomere depleted vesicles (Tel-) served as control. Data from n= 3 donors. Scale bars, 10, 5 or 1 μm as shown throughout. Error bars indicate S.E.M. throughout. Statistical tests, Supplementary table 1.

Europe PMC Funders Author Manuscripts

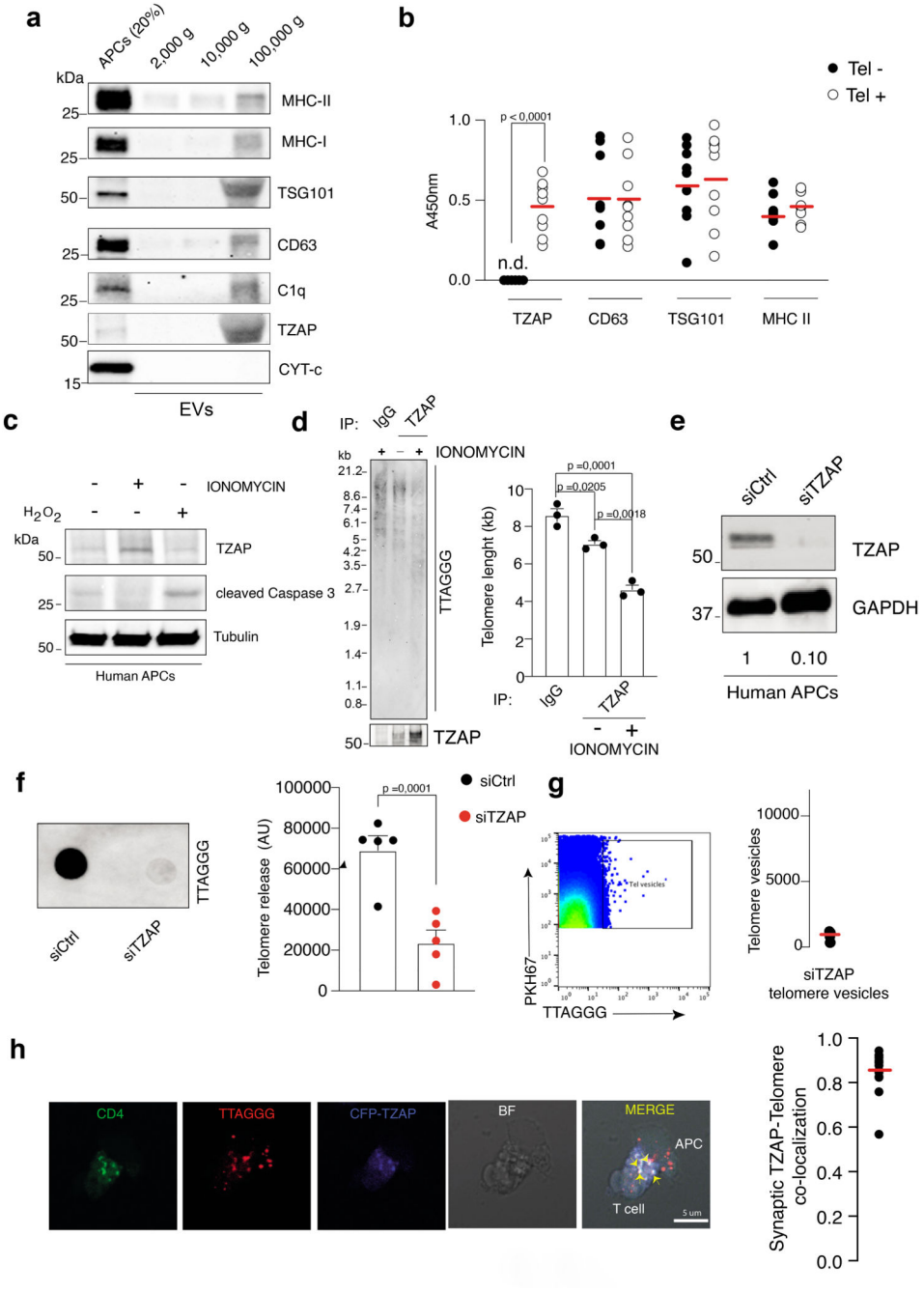

Figure 3. TZAP is required for telomere transfer.

(**a**) Composition of telomere vesicles derived from ionomycin stimulated APCs by immunoblotting. APC lysates (20%), input control. Representative of n= 3 donors. (**b**) Protein cargo analysis in FAVS purified telomere vesicles (TTAGGG^{+} PKH67^{+}; Tel+) or telomere depleted vesicles (TTAGGG^{-} PKH67^{+}; Tel-) by indirect ELISA. Results from n= 9 experiments are shown. (**c**) APCs treated as indicated for 18h were analysed by immunoblot against cleaved caspase 3 as apoptosis marker, and the telomere trimming factor TZAP. Tubulin, loading control. Representative of n= 3 donors. (**d**) Representative

TRF analysis (**left**) and pooled data from (*n*= 3 experiments; **right**) of TZAP dependent telomere trimming *in vitro*. TZAP was immunoprecipitated from APCs cultured with or without ionomycin for 18h and the immunoprecipitates were incubated for additional 18h at 30°C with genomic DNA extracted from resting APCs. TRF analysis determined telomere shortening upon incubation with TZAP but not control IgG immunoprecipitates that was enhanced by ionomycin. (**e**) Immunoblotting validation of TZAP depletion by siRNA nucleofection. Human APCs were transfected with siCtrl or siTZAP for 72h followed by immunoblotting to TZAP. GAPDH, loading control. The numbers indicate quantification of knock-down efficiency. Representative of *n*= 3 experiments. (**f**) Defective telomere vesicle production by TZAP-deficient APCs. APCs were transfected with control siRNA (siCtrl) or silencing TZAP RNA (siTZAP) for 72 hours and stimulated with ionomycin for 18 hours during the 72h culture before telomere vesicle analysis of their ultra-centrifuged supernatants. Representative results (**left**) and pooled data from *n*= 5 experiments (**right**). (**g**) The siTZAP vesicles from one million APCs were counted by FAVS. The red bar indicates mean from *n*= 4 experiments. Donor matched, TZAP-proficient APCs, Fig. 4g-h. (**h**) TZAP transfer at the immune synapse. TZAP-over-expressing APCs (10^6) were conjugated 24h with primary human nonsenescent CD4+ T cells in a 3:1 ratio in the presence of antigen pool then analysed by IF-FISH. Representative of *n*= 3 donors. Error bars indicate S.E.M. throughout. Statistical tests, Supplementary table 1.

Europe PMC Funders Author Manuscripts

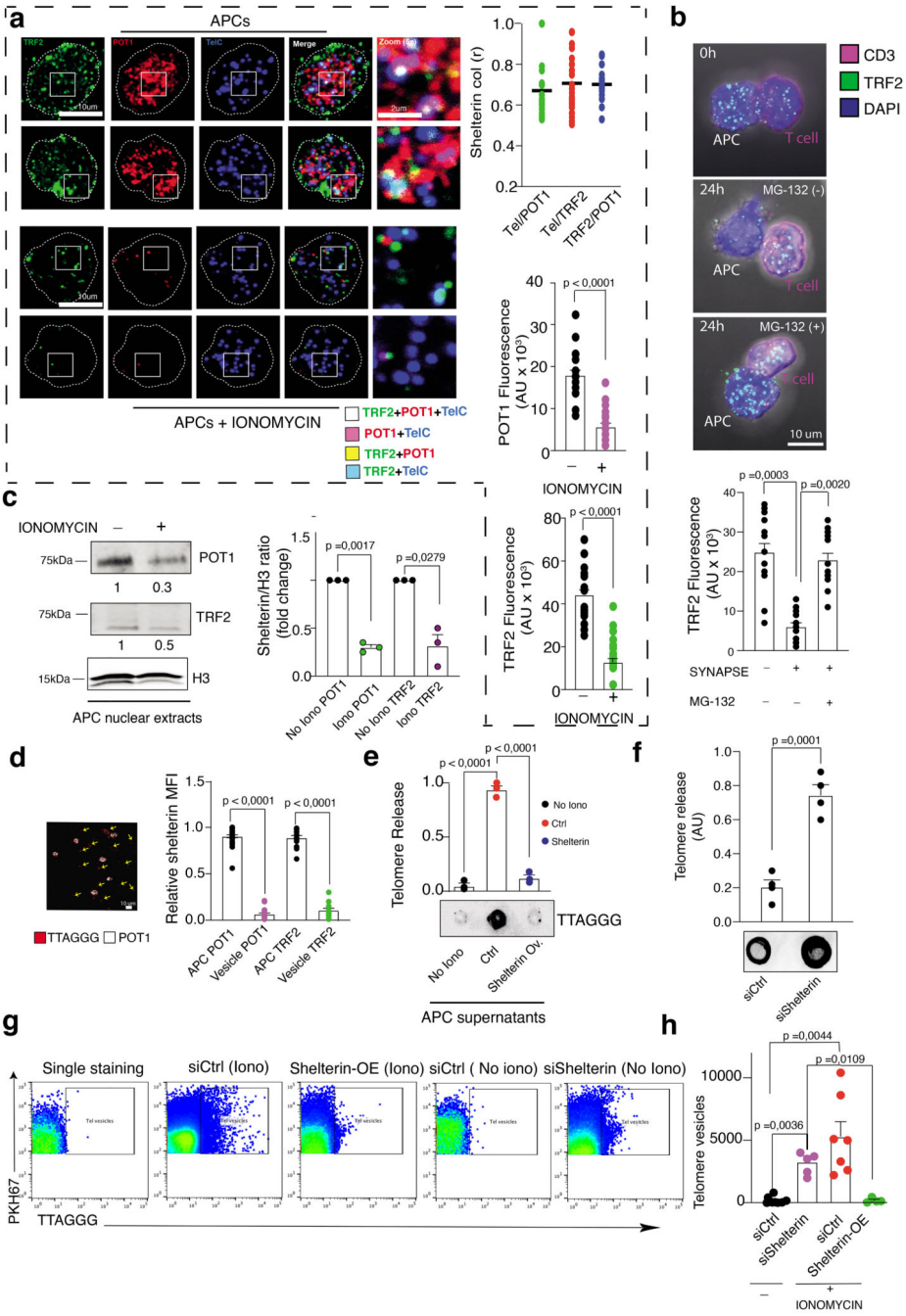

Figure 4. APCs dismantle shelterin to donate telomeres.

(**a**) Activated APCs lose shelterin asssessd by IF-FISH of shelterin proteins in primary human APCs cultured without (**top two left**) or with (**bottom two left**) ionomycin (0.5 μg/mL) for 18h. Results from *n*= 4 donors. Co-localization scores, (**top right**). Shelterin relative mean fluorescence intensity, **middle and bottom right**. Scale bar, 2 μm. (**b**) Representative immunoblot (**left**) and pooled data (*n*= 3 donors**; right**) from APC nuclear extracts treated with (+) or without (-) ionomycin quantification. H3, loading control. (**c**) Representative images (**left**) and quantification (**right**) from *n*= 3 donors of TRF2 by

immunofluorescence in primary human APCs left either untreated, or pre-incubated with the proteasome inhibitor MG-132 (1μM) then conjugated with nonsenescent $CD4^+$ T cells for 24h in the presence of antigen pool. Scale bar, 10 μm. (**d**) APCs donate shelterin-devoid telomeres. TelC-labelled APCs were activated with ionomycin for 18h, then analysed by IF to POT1. Arrows indicate 'shelterin-devoid' telomeres released by APCs. Quantification of TRF2 is also shown (n= 3 donors). Scale bar, 10 μm. (**e**) Shelterin over-expression arrests telomere release from activated APCs. Telomere dot blot on BrDU immunoprecipitates from APCs transduced with mock or shelterin overexpressing (Shelterin OE) vectors to TRF2 + POT1, then activated with or without ionomycin for 18h (n= 3 experiments). (**f**) Spontaneous release of telomere vesicles from supernatants of resting primary human APCs transfected with siCtrl or siTRF2 plus siPOT1 during a 72h culture. Quantification from n= 4 independent experiments (**top**) and representative telomere dot-blot (**bottom**). (**g**) Representative FAVS profiles and quantifications of telomere vesicles released by 10^6 ionomycin activated APCs modified as indicated. TTAGGG, telomeres; PKH67, lipid dye used for vesicle detection. For quantifcation, each dot is an individual donor. (**h**) Quantificaiton of (**g**). N = 7 (siCtrl); n= 5 (siShelterin), n= 7 (siCtrl iono); n= 4 (Shelterin-OE iono). Error bars indicate S.E.M. throughout. Statistical tests, Supplementary table 1.

Europe PMC Funders Author Manuscripts

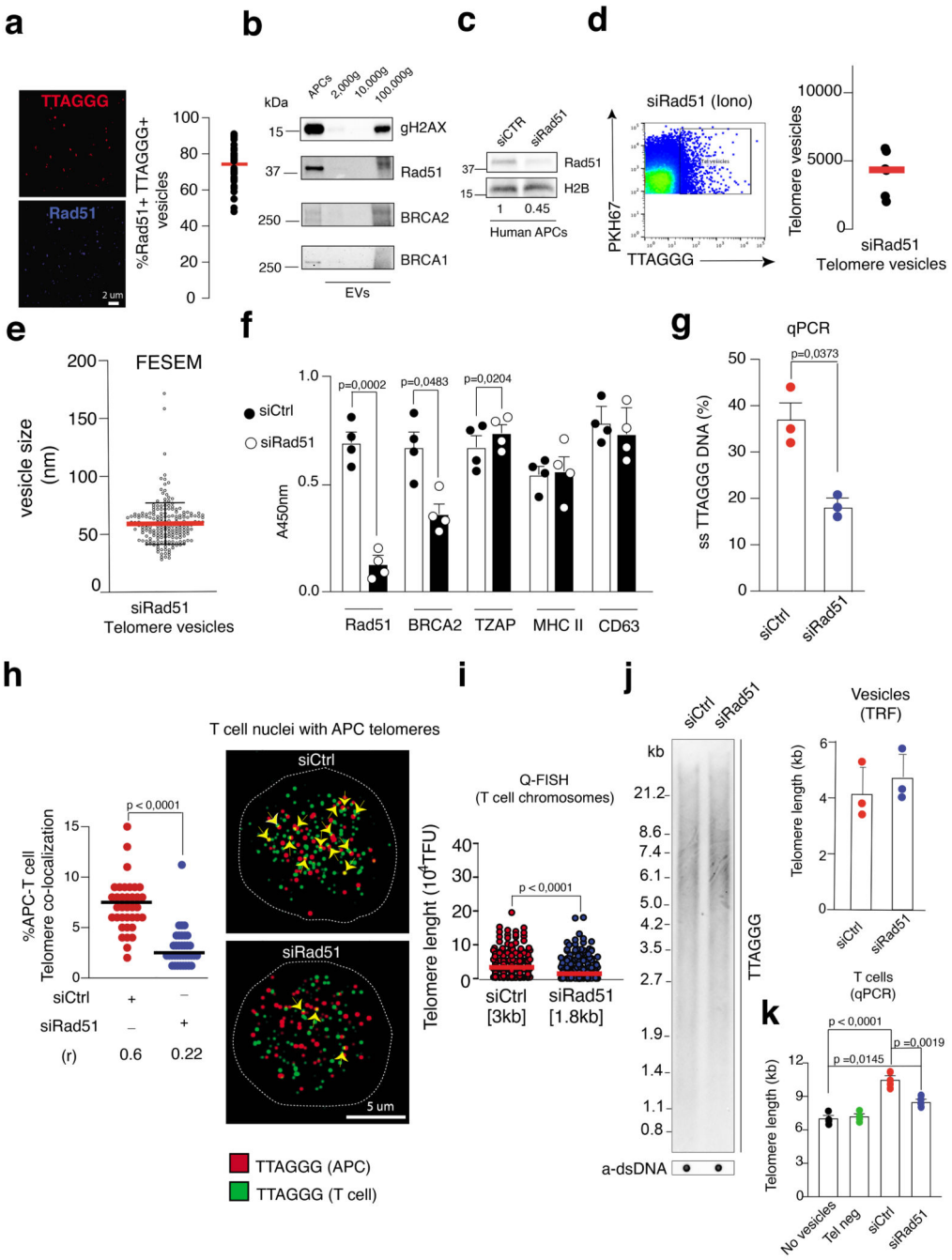

Figure 5. Defective recombinogenic potential in Rad51-deficient telomere vesicles.

(**a**) Presence of Rad51 assessed by IF in APC vesicles upon 18h ionomycin activation. Representative results (**left**) and pooled data from forty-two microscopy fields are shown (n=3 experiments; **right**). Scale bars, 2 μm. (**b**) DNA damage factors in extracellular vesicles derived by sequential centrifugation of APC supernatants as in (**a**). APCs, whole cell lysate control (n=3 experiments). (**c**) Validation of Rad51 deficiency by siRNA treatments in primary human APCs. Histone H2B, loading control. Representative of n=3 donors. (**d**) Release of telomere vesicles by 10^6 Rad51-deficient APCs (siRad51; **left**) assessed by FAVS

Europe PMC Funders Author Manuscripts

(n=6 donors). (**e**) Size of siRAd51 telomere vesicles by FESEM. Two-hundred vesicles were enumerated from *n*=3 experiments (three donors). (**f**) Protein cargo in FAVS purified siRad51 or siCtrl telomere vesicles by ELISA (*n=4* experiments). (**g**) siCtrl and siRad51 vesicles were assessed by QAOS (*n*=3 experiments). (**h**) Role of vesicular Rad51 in APC-T cell telomere colocalization. Cell-free supernatants containing red fluorescent siCtrl or siRad51 APC-telomere vesicles were transferred into T cells with green telomeres that were live-labelled in the same manner prior to telomere transfer. Analysis was carried 24h later. Arrowheads, APC-T cell telomere co-localization. Only green signals are endogenous T cell telomeres. Scale bar, 5 μm. Representative results (**left**) and thirty-six cells pooled from *n=6* experiments (six donors) for each treatment **(right**). (**i**) Metaphase Q-FISH showing defective elongation of individual T cell chromosome ends upon transfer of telomere vesicles derived from Rad51-deficient APCs (siCtrl, 370 and siRad51, 378 from *n=6* experiments). (**j**) siCtrl and siRad51 vesicles were assessed by TRF (*n*= 3 experiments). (**k**) Reduced fusion (elongation) between siRad51 telomere vesicles and T cell telomeres. Nonsenescent (10^6) $CD4^+$ T cells were treated with five-thousands FAVS-purified siCtrl or siRad51 APC-derived telomere vesicles (Tel^+) and total nuclear T cell extracts were analysed by qPCR 48h later (*n*= 3 experiments). Five-thousands telomere depleted vesicles (Tel^-) were also transferred as control. Error bars indicate S.E.M. throughout. Statistical tests, Supplementary table 1.

Europe PMC Funders Author Manuscripts

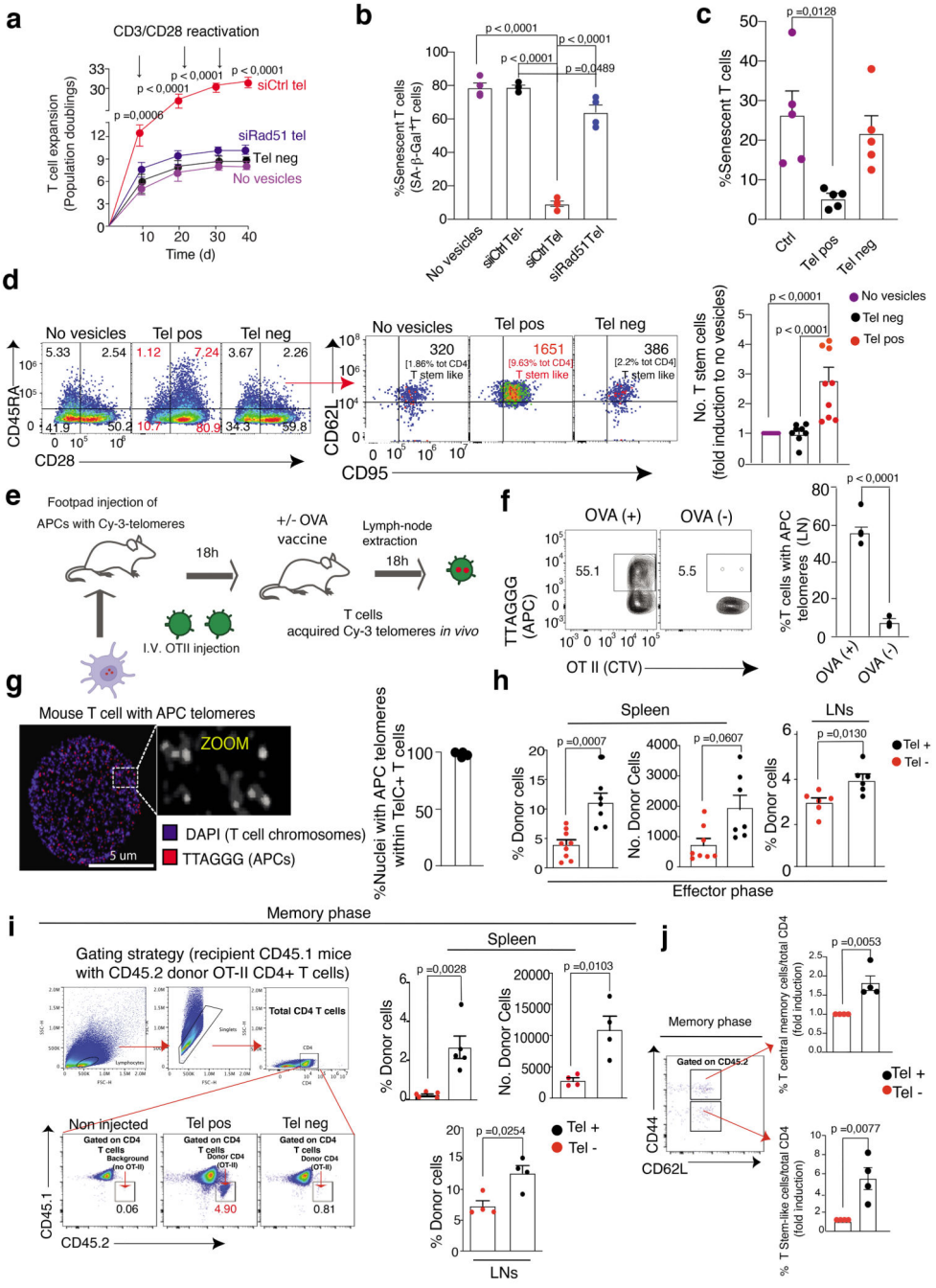

Figure 6. Generation of long-lasting immunity by telomere transfer.

(**a**) Population doublings of nonsenescent CD4$^+$ T cells activated as indicated and treated once with siCtrl or siRad51 telomere vesicles at the start of the culture for 39 days (n= 3 donors). (**b**) Lack of beta-galactosidase activity in nonsenescent CD4$^+$ T cells activated with anti-CD3 plus anti-CD28 for ten days and treated with 1,000 siCtrl or siRad51 telomere vesicles (n= 4 donors). (**c**) Prevention of senescent T cell generation by telomere transfer from naïve CD4$^+$ T cells activated by anti-CD3 and anti-CD28 and treated with 250 telomere vesicles for fifteen days (n= 5 donors). (**d**) Generation of CD62L$^+$ CD95$^+$ stem-like

memory T cells from naïve $CD4^+$ T cells during the fifteen day culture (*n*= 8 experiments). (**e**) Demonstration of *in vivo* telomere transfer, experimental design. (**f**) Presence of APC telomeres among the transferred OT II T cells (*n*=3 mice). (**g**) APC telomeres (red) into the recipient T cell nuclei after *in vivo* telomere transfer (*n*=3 mice). Scale bar, 5 μm. (**h**) Naïve CD45.2 OT-II T cells were separated into Tel^+ versus Tel^- following synaptic telomere transfer from APCs pulsed with OVA, then injected into wild type CD45.1 recipients, then immunized with OVA with assessment after five days. Expansion of transferred CD45.2 OTII Tel^+ T cells in both spleen (%donor spleen Tel+ *n* = 7 mice and Tel- *n=9* mice*;* and no. donor spleen Tel+ *n*= 5 mice and Tel- *n*= 6 mice) and lymph nodes (*n*= 6 mice per group). (**i**) Gating strategy (**left**) and data (**right**) showing enhanced *in vivo* presence of CD45.2 OTII Tel^+ T cells derived and injected as in (**g**), with a second vaccination of recipients after forty days and assessment of CD45.2 OTII T cells fifty days later: data are from n = 5 mice (%donor spleen cells) or n= 4 mice per group. (**j**) Induction of $CD95^+$ stem-like CD45.2 OT II T cells, and that of central memory CD45.2 OT II T cells as in (**i**). Data from *n*= 4 mice per group. Error bars indicate S.E.M. throughout. Statistical tests, Supplementary table 1.

Europe PMC Funders Author Manuscripts

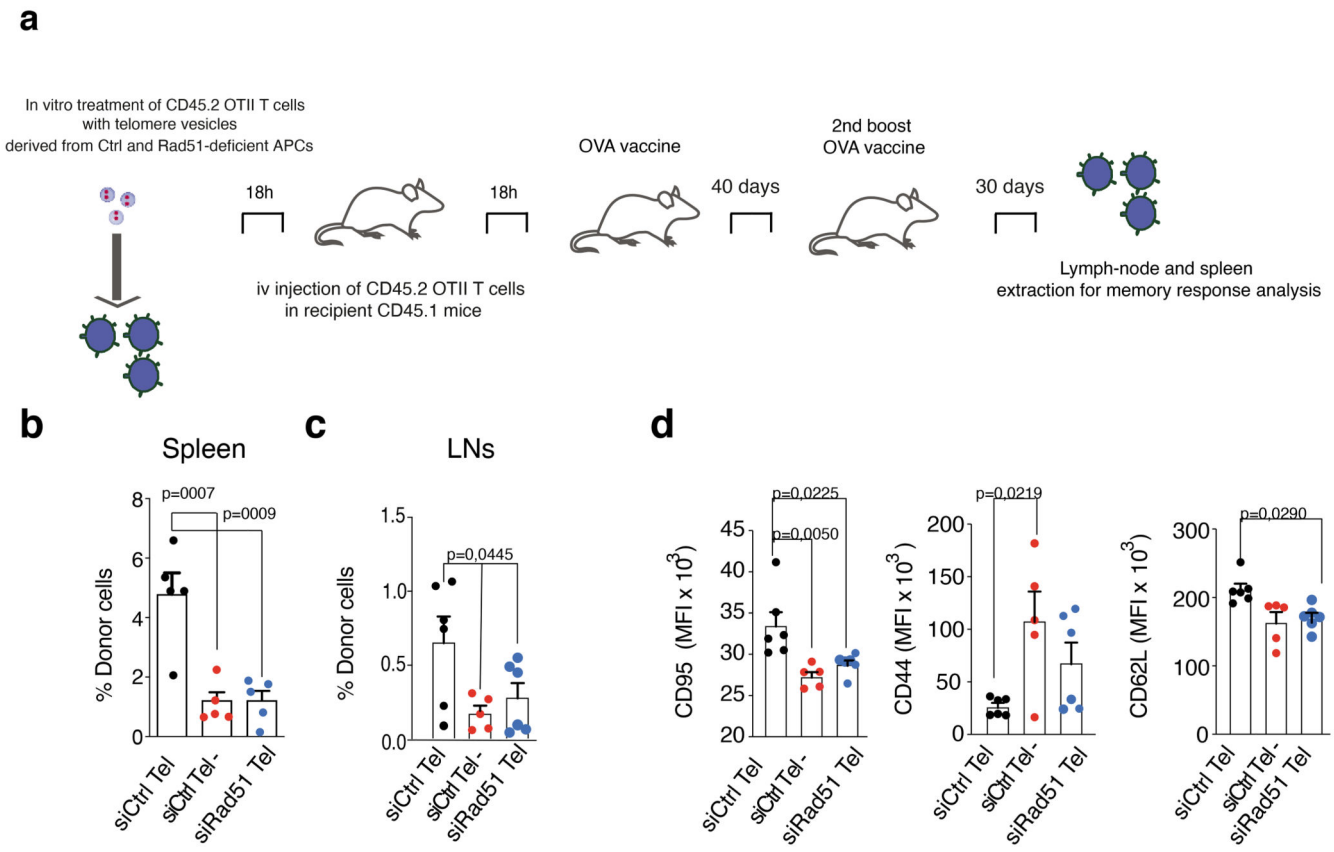

Figure 7. Vesicular Rad51 is required for the longevity effect of the telomere vesicles.

(**a**) Naïve CD45.2 OT II ($CD4^+$) T cells were treated with 500 telomere vesicles from siRNA control transfected APCs (siCtrl), Rad51 depleted vesicles (siRad51 tel) or telomere depleted vesicles (Tel-) from siRNA transfected APCs (congenic CD3-depleted splenocytes) for 24h then transferred into recipient CD45.1 mice. Mice were challenged with OVA 18h later, rested for 40 days, followed by OVA restimulation, rested for another 30 days followed by assessment of presence of donor T cells by flow-cytometry. Analysis was carried out 70 days post-transfer to assess percentage of donor CD45.2 OTII T cells in the spleen (**b**) and (**c**) lymph nodes of recipient CD45.1 mice. (**d**) Phenotypic analysis of splenic CD45.2 OTII ($CD4^+$) T cells 70 days in adoptive transfer experiments described in (**a**) that is assessment of memory response 70 days after telomere transfer. Data are from n= 5 mice (**b**), n= 6 mice (**c**) and for (**d**) n= 6 mice (CD95, all conditions; CD44 siCtrl Tel and siRad51 Tel; CD62L siCtrl Tel and siRad51 Tel) $n = 5$ mice (CD44 siCtrl Tel-; and CD62L siCtrl tel-). Each dot is an individual animal. Error bars indicate S.E.M. throughout. Statistical tests, Supplementary table 1.

Europe PMC Funders Author Manuscripts

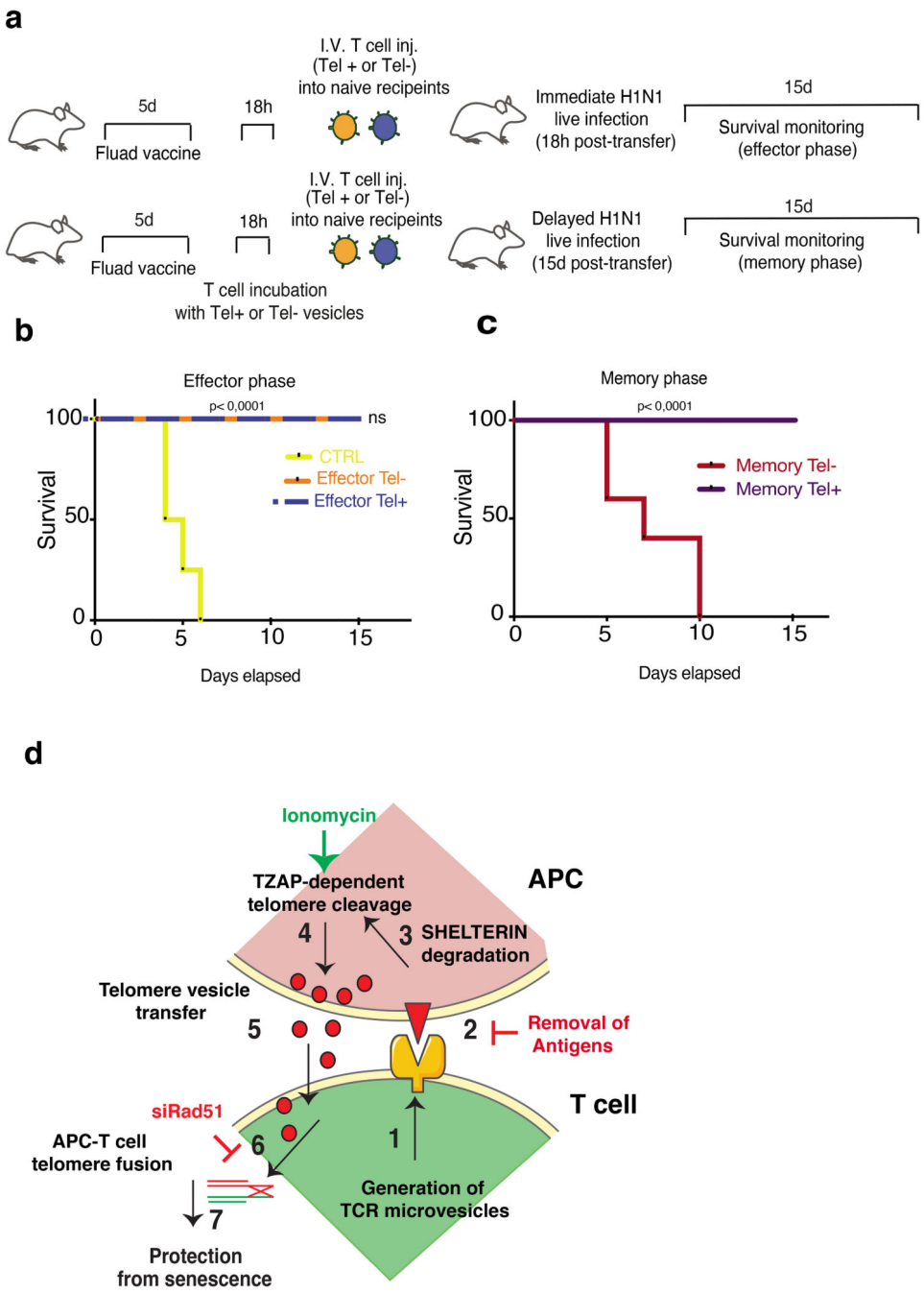

Figure 8. Role of telomere vesicle transfer in immune defense.

(**a**)Experimental design. Mice were vaccinated with FLUAD (1:20 of the human dose) and sacrificed after five days, to derive splenic $CD4^+$ T cells that had been primed by the vaccine. Primed $CD4^+$ T cells were incubated with 5,000 vesicles containing telomeres (Tel+ ves) or 5,000 depleted of telomeres (Tel- ves) obtained from ionomycin activated APCs of congenic origin not exposed to FLUAD for 18h then adoptively injected into recipient naïve C57BL/6J mice (*n*= 5 animals per group). Control mice (*n=4* animals) were injected with T cells from C57BL/6J mice not primed with the FLUAD vaccine. Recipient

Europe PMC Funders Author Manuscripts

mice were then early (after 18 hours) and delayed (after 15 days) infected with H1N1 flu virus ($3.5x10^5$ PFU). Survival was monitored for fifteen days and clinical score was recorded throughout. Mice (*n=5* animals per group) were sacrificed when a clinical score was equal or above 10, or in any case severe dyspnea was observed. Clinical scoring for sign of illness was performed as described in Methods. (**b**) Survival of mice receiving either CD4+ T cells with APC telomere vesicles (Tel^+) or with telomere depleted vesicles (Tel^-) from FLUAD-primed congenic donors as in panel (**a**) and infected immediately. Ctrl, animals injected with T cells that had not been exposed to the vaccine (**yellow line**). (**c**) Survival of mice receiving either Tel^+ or Tel^- T cells as in (**b**) and infected 15 days later. Statistical tests, Supplementary table 1.